Journal Pre-proofs

Source Apportionment of Fine Particulate Matter in a Middle Eastern Metropolis, Tehran-Iran, Using PMF with Organic and Inorganic Markers

Sepideh Esmaeilirad, Alexandra Lai, Gülcin Abbaszade, Jürgen Schnelle-Kreis, Ralf Zimmermann, Gaëlle Uzu, Kaspar Daellenbach, Francesco Canonaco, Hossein Hassankhany, Mohammad Arhami, Urs Baltensperger, André S.H. Prévôt, James J. Schauer, Jean-Luc Jaffrezo, Vahid Hosseini, Imad El Haddad

PII: S0048-9697(19)35322-7
DOI: https://doi.org/10.1016/j.scitotenv.2019.135330
Reference: STOTEN 135330

To appear in: *Science of the Total Environment*

Received Date: 22 August 2019
Revised Date: 30 October 2019
Accepted Date: 31 October 2019

Please cite this article as: S. Esmaeilirad, A. Lai, G. Abbaszade, J. Schnelle-Kreis, R. Zimmermann, G. Uzu, K. Daellenbach, F. Canonaco, H. Hassankhany, M. Arhami, U. Baltensperger, A.S.H. Prévôt, J.J. Schauer, J-L. Jaffrezo, V. Hosseini, I. El Haddad, Source Apportionment of Fine Particulate Matter in a Middle Eastern Metropolis, Tehran-Iran, Using PMF with Organic and Inorganic Markers, *Science of the Total Environment* (2019), doi: https://doi.org/10.1016/j.scitotenv.2019.135330

Source Apportionment of Fine Particulate Matter in a Middle Eastern Metropolis, Tehran-Iran, Using PMF with Organic and Inorganic Markers

Sepideh Esmaeilirad[a], Alexandra Lai[b], Gülcin Abbaszade[c], Jürgen Schnelle-Kreis[c], Ralf Zimmermann[c, d] Gaëlle Uzu[e], Kaspar Daellenbach[f,1], Francesco Canonaco[f], Hossein Hassankhany[g], Mohammad Arhami[h], Urs Baltensperger[f], André S. H. Prévôt[f], James J. Schauer[b], Jean-Luc Jaffrezo[e], Vahid Hosseini[a*], Imad El Haddad[f]**

[a] Department of Mechanical Engineering, Sharif University of Technology, Azadi Ave., Tehran 11155-9567, Iran

[b] Environmental Chemistry & Technology Program, University of Wisconsin-Madison, Madison, WI, USA

[c] Joint Mass Spectrometry Centre, Comprehensive Molecular Analytics, Helmholtz Zentrum München, 85764 Neuherberg, Germany

[d] Joint Mass Spectrometry Centre, Chair of Analytical Chemistry, University of Rostock, 18059 Rostock, Germany

[e] Université Grenoble Alpes, CNRS, IRD, INP, IGE, UMR 5001,38000 Grenoble, France

[f] Laboratory of Atmospheric Chemistry, Paul Scherrer Institute (PSI), 5232 Villigen-PSI, Switzerland

[g] Tehran Air Quality Control Company, Tehran Municipality, Tehran, Iran

[h] Department of Civil Engineering, Sharif University of Technology, Azadi Ave., Tehran 11155-9313, Iran

[1] now at: Institute for Atmospheric and Earth System Research/Physics, Faculty of Science, University of Helsinki, P.O. Box 64, 00014, Helsinki, Finland

[*] Corresponding author: V. Hosseini, Department of Mechanical Engineering, Sharif University of Technology, Azadi Avenue, P.O. Box 11155-9567, Tehran, Iran, Tel: +98(21) 66165501-2, Email: vhosseini@sharif.edu

[**] Corresponding author: I. El Haddad, Laboratory of Atmospheric Chemistry, Paul Scherrer Institute, Forschungsstrasse 111, OFLA/004, 5232 Villigen PSI, Switzerland, Tel.: +41(56) 3102995, Email: imad.el-haddad@psi.ch

ABSTRACT

With over 8 million inhabitants and 4 million motor vehicles on the streets, Tehran is one of the most crowded and polluted cities in the Middle East. Frequent exceedances of national daily $PM_{2.5}$ limit have been reported in this city during the last decade, yet, the chemical composition and sources of fine particles are poorly determined. In the present study, 24-hour $PM_{2.5}$ samples were collected at two urban sites during two separate campaigns, a one-year period from 2014 to 2015 and another three-month period at the beginning of 2017. Concentrations of organic carbon (OC), elemental carbon (EC), inorganic ions, trace metals and specific organic molecular markers were measured by chemical analysis of filter samples. The dominant mass components were organic matter (OM), sulfate and EC. With a 20% water-soluble organic carbon (WSOC), the predominance of primary anthropogenic sources (i.e. fossil fuel combustion) was anticipated. A positive matrix factorization (PMF) analysis using the ME-2 (Multilinear Engine-2) solver was then applied to this dataset. 5 factors were identified by Marker-PMF, named as traffic exhaust (TE), biomass burning (BB), industries (Ind.), nitrate-rich and sulfate-rich. Another 4 factors were identified by Metal-PMF, including, dust, vehicles (traffic non-exhaust, TNE), industries (Ind.) and heavy fuel combustion (HFC). Traffic exhaust was the dominant source with 44.5% contribution to total quantified $PM_{2.5}$ mass. Sulfate-rich (24.2%) and nitrate-rich (18.4%) factors were the next major contributing sources. Dust (4.4%) and biomass burning (6.7%) also had small contributions while the total share of all other factors was less than 2%. Investigating the correlations of different factors between the two sampling sites, showed that traffic emissions and biomass burning were local, whereas dust, heavy fuel combustion and industrial sources were regional. Results of this study indicate that gas- and particle-phase pollutants emitted from fossil fuel combustion (mobile and stationary) are the principal origin of both primary and secondary fine aerosols in Tehran.

Keywords: $PM_{2.5}$; PMF; metals; organic markers; regional/local sources.

1. Introduction

Air pollution is one of the major environmental challenges in metropolitan cities of developing countries, owing to its adverse effects on public health. According to the World Health Organization about 90% of people around the world live in cities that do not comply with the WHO air quality guidelines (WHO 2016). Although air pollution may have a natural component, e.g. desert dust, anthropogenic activities are known to be the main driver of air pollution in cities. High population growth, increasing urbanization and industrialization in Asian countries have led to increases in the level of atmospheric pollutants. Particulate matter (PM) is among the most important air pollutants and exposure to high concentrations of particles with aerodynamic diameters less than 2.5 μm ($PM_{2.5}$) can cause cardiovascular and respiratory diseases (Habre et al., 2014; HEI, 2013; Koton et al., 2013; Mohseni Bandpi et al., 2017; Van Ryswyk et al., 2014). A study of the global burden of disease attributed to ambient air pollution reported that ambient $PM_{2.5}$ was the fifth-ranking mortality risk factor in 2015, causing 4.2 million deaths (Cohen et al., 2017). For designing efficient mitigation strategies in any area, it is important to identify its main sources of ambient PM.

Since particulate matter originates from diverse sources, it contains a wide range of chemical species. Organic carbon (OC) and elemental carbon (EC) are major PM components. While EC originates from combustion processes, OC in the atmosphere comes either from direct emissions (primary organic carbon, POC) or chemical conversion of organic gases in the atmosphere (secondary organic carbon, SOC) (Hallquist et al., 2009). Depending on the location and season, common urban sources of POC and SOC precursors are vehicular exhaust, industrial emissions, biogenic emissions, and coal and biomass burning (e.g. Alves et al., 2012; Huang et al., 2019; Vlachou et al., 2018; Waked et al., 2013; Wang et al., 2015). Primary OC is a mixture of numerous organic compounds; including n-alkanes, polycyclic aromatic hydrocarbons (PAHs) and their derivatives, hopanes, sterols, anhydrous

sugars, etc. Many of these compounds are known as source markers (Cass, 1998; Simoneit et al., 1999). Except near emission sources, a great share of OC mass (almost 72% ± 21%) is attributed to secondary organic aerosol (SOA) (Jimenez et al., 2009), whose composition and sources remain highly uncertain. A large share of OC can also have primary biogenic origin, particularly in summer (Samaké et al, 2019). Other major components of $PM_{2.5}$ are inorganic ions, including sulfate, nitrate and ammonium, which are produced from secondary reactions of gaseous precursors and subsequent partitioning into the particle phase (Hidy, 1994; Ying, 2011). Besides these major components, $PM_{2.5}$ includes trace concentrations of metals and metalloids. Some of these elements can be considered as useful markers of sources such as dust, break and tire abrasion, industrial activities and fuel oil combustion (Charron et al., 2019; Harrison et al., 2012; Peltier et al., 2010; Querol et al., 2007).

Due to the diversity of PM chemical components and their origins, it is important to identify specific PM sources in different environments. Receptor modeling uses the chemical fingerprints of air pollutants to identify and apportion their contributing sources. These models use measured data of PM chemical composition and their corresponding uncertainty to evaluate the contributions of emission sources to atmospheric PM pollution. Common receptor models can be categorized into univariate models, such as chemical mass balance (CMB), and multivariate models, such as principal component analysis (PCA), positive matrix factorization (PMF), and the US EPA's Unmix model. While these modeling techniques have been extensively used in developed countries for PM source apportionment purposes, similar studies in developing areas, especially those in the Middle East are quite sparse. Nevertheless, there are a few number of studies focusing on chemical characterization and source apportionment of PM in the Middle Eastern countries, such as Iraq (Engelbrecht and Jayanty, 2013; Hamad et al., 2015), Israel, Jordan and Palestine (Heo et al., 2017; von Schneidemesser et al., 2010), Kuwait (Al-Dabbous and Kumar, 2015; Alolayan et al., 2013),

Lebanon (Waked et al., 2013), Saudi Arabia (Alharbi et al., 2015; Bian et al., 2018; Khodeir et al., 2012; Nayebare et al., 2016; 2018), and Turkey (Koçaka et al., 2011; Tecer et al., 2012).

Tehran, capital of Iran and a major metropolis in the Middle East, has been suffering from severe air pollution conditions for many years (Hosseini and Shahbazi, 2016). It has a population of 8.5 million, which can reach above 12.5 million during the day due to people commuting from nearby cities. During the past decade, Tehran has frequently experienced episodes of high air pollution during winter, or dust phenomena during summer (Alizadeh-Choobari, et al., 2016; Givehchi et al., 2013; Jaafari et al., 2017). Supplemental Figure S1 (a) presents a comparison of 24-hour $PM_{2.5}$ levels observed in Tehran and other cities worldwide. This bar graph places Tehran among the polluted cities in the world, which violate the WHO international air pollution standards. Tehran $PM_{2.5}$ pollution is mostly attributed to rapid industrialization and the large number of motor vehicles (usually with outdated emission standards) (Shahbazi et al., 2016). The characteristic topography of Tehran aggravates the air pollution situation. The prevailing westerly and southerly winds, transport pollutants from industrial zones towards the city and the mountain barriers lying to the north and east of Tehran hinder the natural wind dilution of the pollutants, resulting in a polluted condition, particularly in central and eastern parts of the city. Studies of the chemical composition and sources of $PM_{2.5}$ in Tehran are scarce. Only recently have a few studies been conducted, with a focus on inorganic ions and elements (Arhami et al., 2017; Arhami et al., 2018; Taghvaee et al., 2018). Mobile sources (light and heavy duty vehicles), secondary aerosols and dust are among the most important $PM_{2.5}$ sources identified by these studies. Results of the current study and those of the past studies will be compared in section 4.2.

PMF has been widely used to apportion PM sources around worldwide. However, most of these analyses were carried out on organic/elemental carbon (OC/EC) and inorganic species

(trace elements and water-soluble ions). Very few PMF studies have focused on organic molecular markers (Bae et al., 2019; Callén et al., 2014; Dutton et al., 2010; Gupta et al., 2018; Heo et al., 2013; Wang et al., 2015) or have combined both organic and inorganic tracers (Bozzetti et al., 2017; Pateraki et al., 2019; Salameh et al., 2018; Vossler et al., 2016; Waked et al., 2014). In the present study, the chemical constituents and sources of ambient $PM_{2.5}$ samples, collected at two sites in central Tehran and during two separate campaigns were investigated. PMF was applied to inorganic and organic markers to identify the source profiles and their contributions. This is the first comprehensive PMF study of $PM_{2.5}$ sources in Tehran, which employs an extensive data set of chemical species (organic molecular markers and trace elements) rarely considered together. The findings provided by this study can be beneficial to policy-makers in order to adjust the air pollution control regulations and improve the air quality in Tehran and may be applied to other major cities in the Middle East.

2. Methods

2.1. Sites description and sampling campaigns

24-hour $PM_{2.5}$ samples were collected during two separate campaigns. In the first campaign (designated by "Campaign_1"), a yearly cycle of sample collection took place from February 2014 to February 2015 and filter samples were collected every 6 days. The second campaign (designated by "Campaign_2") was more intensive and filter samples were collected every other day from late-January 2017 to mid-April 2017. In Campaign_1, the sampling station was set up on the roof of an air quality monitoring station at Sharif University of Technology campus in the central-west part of Tehran ("Sharif" site, 35.7038° N and 51.3490° E). In Campaign_2, two sampling sites were selected, one of which was the same as Campaign_1 and the other was located inside a crisis management Headquarters in the central-east part of Tehran ("Setad" site, 35.7271° N and 51.4312° E). These two sites are approximately 8

kilometers apart. Both sampling sites are part of Tehran's air quality monitoring network and are operated by Tehran Air Quality Control Company. These monitoring stations record the hourly concentrations of PM_{10}, $PM_{2.5}$, CO, NO_2, SO_2 and O_3. They are located in residential areas and are surrounded by major streets (Azadi and Motahari) as well as several local streets. They are affected by a mixture of common urban sources, such as vehicular traffic, road dust re-suspension, local commercial/industrial emissions, and construction activities. Thus, the selected sites are representative of a general residential location in urban areas of Tehran. Supplemental Figure S1 (b) shows the location of the two sampling sites in Tehran.

In Campaign_1, two sets of samples were collected concurrently on quartz fiber filters (47 *mm* diameter, Whatman Inc.) and Teflon filters (47 *mm* diameter, PTFE Teflon, Pall Life Science) using two low-volume ambient air samplers (PQ200 by BGI, Inc., USA). The samplers were operated at a flow rate of 16.7 *lpm* and equipped with a volumetric flow controller. In Campaign_2, only quartz fiber filters (47 *mm* diameter, Pall Life Science) samples were collected at each site, using the same low-volume samplers as in Campaign_1. In both campaigns, low volume air samplers were run for 24 hours, with a $PM_{2.5}$ cyclone installed at the inlet. Quartz filters were baked before sampling at 550°*C* for at least 12 hours. Field blanks were collected for every 5-10 sets of samples (depending on the sampling frequency of the campaign). A total of 116 $PM_{2.5}$ samples were collected during the two study campaigns (51 samples from Campaign_1, 35 samples from Campaign_2, Setad site and 30 samples from Campaign_2 Sharif site). All samples were placed and sealed in polystyrene Petri dishes and stored frozen before analysis in order to prevent evaporation of volatile components. Since no backup filters were used during the sampling procedure, negative and positive artifacts, caused by desorption and adsorption of semi-volatile vapors, respectively, could not be verified.

2.2. Chemical analysis

Organic and elemental carbon (OC and EC) concentrations in both campaigns were determined using a 1 cm^2 punch of each individual quartz filter by a Thermal/Optical Transmittance technique (TOT, Sunset laboratory, Forest Grove, Oregon), through the NIOSH protocol (Birch and Cary, 1996; Schauer et al., 2003; Villalobos et al., 2015). Inorganic ions, including SO_4^{2-}, NO_3^-, NH_4^+, Cl^- and Ca^{2+}, were analyzed by ion chromatography (IC), after extracting one-quarter of each quartz fiber filter in high purity water, by means of a Dionex ICS 1100 and 2100 (Villalobos et al., 2015). The water-soluble carbon (WSOC) content of the samples was measured in the same extract by a Shimadzu TOC-5000A liquid analyzer (Decesari et al., 2005). These analyses were performed at the Water Science and Engineering Laboratory and the Wisconsin State Laboratory of Hygiene at the University of Wisconsin-Madison for samples from both campaigns.

Major metals (including Al and Fe), as well as trace metals (including Ti, Mn, Ni, V, Cu, As, Zn, Rb, Mo, Cd, Sb and Pb) were analyzed by inductively coupled plasma mass spectrometry (ICP/MS), after an acidic digestion of a fraction of the samples using a mixture of inorganic acids. Samples from Campaign_1 were measured at Water Science and Engineering Laboratory (Lough et al., 2005) and samples from Camapign_2 were measured at Institut des Géosciences de l'Environnement, CNRS at Grenoble, France (Waked et al., 2014). Organic marker compounds were analyzed using an in-situ derivatization thermal desorption gas chromatography time of flight mass spectrometry (IDTD-GC-MS) method. Details of this method are described elsewhere (Orasche, et al., 2011). The quantified organic markers, listed in the Supplemental Table S1, include 13 polycyclic aromatic hydrocarbons (PAHs), 3 anhydrous sugars, 12 hopanes and 11 n-alkanes. Organic molecular marker measurements were performed at Helmholtz Zentrum München, German Research Center for Environmental Health (GmbH).

2.3. PMF analysis

PMF was developed by Paatero and Tapper (1994) in order to develop a new method for the analysis of multivariate data that resolved some limitations of the PCA. It employs *m* observations of *n* measured quantities, $x_{i,j}$, at a receptor site and it derives *p* individual source components, *f*, and their time-dependent intensities, *g*, plus a residual term $e_{i,j}$:

$$x_{i,j} = \sum_{k=1}^{p} (g_{i,k} \cdot f_{k,j}) + e_{i,j}. \quad (1)$$

The solution is a weighted iterative least squares fit minimizing *Q* as in Eq. (2), where the known measurement uncertainties $\sigma_{i,j}$ for the values $x_{i,j}$ are used to determine the weights of the residuals $e_{i,j}$:

$$Q = \sum_i \sum_j \left(\frac{e_{i,j}}{\sigma_{i,j}} \right)^2. \quad (2)$$

Such minimization is performed with the constraint of non-negative values for source profiles (**F**) and their contribution (**G**). The uncertainty matrix was estimated as follows:

$$\sigma_{i,j} = \sqrt{(\mathrm{RR} \times x_{i,j})^2 + (\mathrm{LOD})^2}. \quad (3)$$

Here, LOD denotes the limit of detection and RR is the relative error based on the measurement repeatability (Rocke and Lorenzato, 1995). For samples below the detection limit we used σ = 4xLOD.

Source apportionment was performed using the ME-2 implementation of PMF (Paatero, 1999) in the SoFi (Source Finder) toolkit (Canonaco et al., 2013) for the IGOR Pro software environment (WaveMetrics, Inc., Portland, OR, USA). PMF-derived solutions are subject to a degree of rotational ambiguity (Paatero et al., 2002). One way to address the rotational ambiguity within the ME-2 solver is with the a-value approach. Here one or more factor

profiles are constrained by the scalar 'a', which determines the extent to which the output profiles are allowed to deviate from the input "anchor" profiles, according to:

$$f_{j,solution} = f_j \pm a \cdot f_j. \quad (4)$$

Here, f represents a row of the profiles matrix and the index j varies between 0 and the number of variables (Canonaco et al., 2013).

Two separate sets of PMF input matrices were constructed for this study. In the first set, data matrix consisted of OC, EC, inorganic ions and organic molecular markers, involving 44 variables (Marker-PMF). The remaining 14 metals were included in a second data matrix (Metal-PMF). The chemical species retained in the input matrices are displayed in the Supplemental Table S2. All data and error matrices contained 109 samples (48 from Campaign_1, 29 from Campaign_2 at Sharif site and 31 from Campaign_2 at Setad site). In the input data matrices of the PMF analysis, concentrations below detection limit were replaced by LOD/2. Based on their signal to noise ratio (*S/N*) (Paatero and Hopke, 2003),"weak" variables (*S/N* between 0.2 and 2.0) were downweighted by increasing their uncertainties by a factor of 3, while "bad" variables (*S/N* < 0.2) were downweighted by increasing their uncertainties by a factor of 10. The PMF algorithm was run in the robust mode in order to dynamically reduce pulling of the solution by outliers.

ME-2 solutions were examined using a number of criteria to select the optimum number of factors and evaluate whether those solutions are environmentally interpretable. We performed unconstrained PMF runs from 2 to 10 factors, each initialized from 30 pseudo-random starting points. The $Q/Q_{expected}$ ratio decreased continuously from 3.9 to 0.8, and from 5.2 to 0.7, respectively for Marker-PMF and Metal-PMF, when the number of factors increased from 2 to 10.

For Metal-PMF, a 4-factor solution ($Q/Q_{expected}$ = 3.5, unexplained variation of all input variables < 25%) was chosen as the most reasonable solution. These factors were identified as: dust, industries, vehicles and heavy fuel combustion. Although the $Q/Q_{expected}$ ratio for a 5-factor solution was 20% lower, the fifth factor resolved by PMF was a splitting of the factor related to industrial emissions. The industrial factors in the 5-factor solution could not be assigned to two specific emission processes and their contributions and profiles highly varied between the different seeds, indicating that several rotations could explain the input data equally. Therefore, we have considered the 4-factor solution as the optimal representation of the data.

For Marker-PMF, to improve the factor separation and direct the PMF solution toward environmentally meaningful rotations, a set of constraints were imposed to a subset of species in the factor profiles. These constraints were chosen based on the prior knowledge of the possible sources and their compositions. The contribution of some species have been fully constrained (a-value = 0) in factor profiles of the Marker-PMF, as follows:

- The contributions of anhydrous sugars, the specific markers of biomass burning (Simoneit et al., 1999), were set to zero in all factors except the biomass burning factor.
- The contributions of all hopanes, markers of traffic exhaust (El Haddad et al., 2009), were set to zero in biomass burning and the factors related to sulfate and nitrate.
- The contributions of EC, a primary fossil fuel combustion tracer, and all organic molecular markers were set to zero in the factors related to sulfate and nitrate.

A 5-factor solution ($Q/Q_{expected}$ = 2.0, unexplained variation of all input variables < 25%) was selected as our best representation of the data. These factors were identified as: industrial emissions, biomass burning emissions, traffic exhaust, nitrate-rich and sulfate-rich.

Investigation of the solutions with a higher number of factors showed a splitting of the traffic exhaust source, which could not be interpreted. A combined Organics + Metals data set was also investigated, but the results could not be interpreted, potentially due to the size of the dataset. Even when factor profiles were constrained, specific sources appeared to be mixed (e.g. traffic exhaust and traffic non-exhaust; industries and heavy fuel combustion) and others were split into factors that could not be ascribed to any specific source (e.g. traffic). Another major issue was the high rotational ambiguity of the PMF, i.e. PMF solutions were highly variable. Thus, the combined PMF results were discarded.

3. Results

3.1. $PM_{2.5}$ major components

Daily average concentrations of $PM_{2.5}$ and PM_{10} during the two study campaigns are reported in Supplemental Figure S2 (a) and (b) for Campaign_1 and Campaign_2, respectively. For the majority of the sampling days, 24-hour concentrations of $PM_{2.5}$ and PM_{10} are above the WHO guidelines during both campaigns. For the first campaign, two pollution episodes can be clearly distinguished. The first episode occurred during cold months, due to a decrease in the boundary layer height and inversion. Similar pollution episodes occurred during Campaign_2 at the two sites, before being interrupted by the New Year holidays when traffic in Tehran significantly drops. The second PM pollution episode occurred during the dry months of the year and was caused by dust storms. A relative increase of the coarse PM fraction (from 50% to 70%, Supplemental Figure S3) and very high levels of PM_{10} characterize this episode. Such pollution episodes are very typical in Tehran, reported to occur every year. $PM_{2.5}$ and PM_{10} levels are generally similar between the two campaigns, with slightly higher levels during Campaign_1, possibly because Campaign_2 does not cover any dust episode (Supplemental Figure S2 (c)). Observed $PM_{2.5}$ concentrations at Setad are

generally lower than that at Sharif (by a factor of 1.24), despite the proximity between the two sites, which indicates that the $PM_{2.5}$ concentration is influenced by local sources. However, $PM_{2.5}$ concentrations are highly correlated at the two sites suggesting that $PM_{2.5}$ variations are mostly driven by regional conditions (e.g. inversion and change in emission patterns due to holidays).

The motor vehicles fleet in Tehran mostly consists of gasoline vehicles, which dominate CO emissions. Increased CO concentrations (Supplemental Figure S4) coincide with the morning and evening rush hours, when there are often heavy traffic jams in the main roads of the city. The same traffic pattern is reflected in the $PM_{2.5}$ and NO_x diurnal evolutions with morning and evening peaks. However, the $PM_{2.5}$ concentration does not decline considerably during the day and the $PM_{2.5}$/CO ratio increases substantially during the middle hours of the day. This observation highlights the important role of non-combustion related $PM_{2.5}$ sources, including secondary PM formation. The similarity between weekday/weekend patterns in Figure S4 suggests that $PM_{2.5}$ sources are similar on weekdays and weekends in Tehran, all dominated by vehicular emissions.

For all the samples, particulate organic matter (OM) was estimated from the measured OC values multiplied by a conversion factor of 1.4 (OM/OC), which is characteristic of urban aerosols dominated by traffic emissions (Turpin and Lim, 2001). The carbonaceous fraction (OM + EC) dominates the quantified $PM_{2.5}$ mass, forming on average 60% of the measured mass (from a minimum of 36% to a maximum of 92%). The inspection of water-soluble organic carbon showed that OC is mostly insoluble, with an average WSOC/OC ratio of 0.2 for both sites and campaigns. This suggests the dominance of water insoluble hydrocarbons from primary emissions, such as fossil fuel combustion. The WSOC/OC ratio in Tehran is much lower than at other locations, where OC is dominated by water soluble secondary species or primary biomass burning emissions (Bozzetti et al., 2017; Daellenbach et al., 2016;

Vlachou et al., 2018). The variations of OC and EC levels are shown in Figure 1 (a) for both campaigns, separately for winter and summer. The average temperature during Camapign_2 was below 10°*C*, thus the entire campaign could be considered as a winter campaign. OC concentrations in the first campaign are higher in winter, ranging from 3.1 to 14.6 $\mu g/m^3$, compared to an average summer concentration of 6.8 $\mu g/m^3$. OC levels in the second campaign are generally higher than the first one.

EC in Tehran, believed to be mostly emitted from heavy-duty diesel vehicles, has a lower yearly variability, with average concentrations of 3.5 $\mu g/m^3$ during both winter and summer. Decreased concentrations of OC and EC in the samples collected during New Year holidays (Figure 1) also imply that these carbonaceous compounds have a traffic origin. Figure 1 (b) compares the OC and EC levels in this study with the observed values during cold and warm months of the year at different parts of the world. Both OC and EC levels in Tehran are higher than the corresponding values in cities of Europe and USA ($2 < C_{OC} < 8$ $\mu g/m^3$; $0.2 < C_{EC} < 2$ $\mu g/m^3$). OC levels in Tehran in winter and summer, as well as EC level in winter are comparable to or lower than the measured values in less developed cities of Asia and South America ($3 < C_{OC} < 18$ $\mu g/m^3$; $1 < C_{EC} < 15$ $\mu g/m^3$). However, the EC level in summer is near to the highest values observed worldwide.

Figure 1 (a) also displays the variation of the sulfate and nitrate levels between different sites and campaigns. Sulfate has an almost constant level throughout the year with a slightly higher mean concentration in summer (4.3 $\mu g/m^3$) compared to winter (3.9 $\mu g/m^3$) (Figure 1 (b)), which is explained by higher photochemical reactivity in summer. On the contrary, average nitrate levels are an order of magnitude higher in winter (1.23 $\mu g/m^3$) than in summer (0.16 $\mu g/m^3$). This is consistent with the enhanced partitioning of nitrate into the particle phase at low temperatures. Mean sulfate concentrations in the second campaign (1.8 $\mu g/m^3$) are generally lower than the first one. For Campaign_2, nitrate levels at Setad (mean = 0.9

$\mu g/m^3$) are comparable with the winter concentrations of Campaign_1, but, Sharif nitrate concentrations (mean = 2.9 $\mu g/m^3$) are higher than all other samples (Figure 1 (a)). A comparison of the sulfate and nitrate concentrations with globally observed values (Figure 1 (b)) shows that these ions have remarkably low levels in Tehran (Europe and USA: $2 < C_{SO_4^{2-}} < 13$ $\mu g/m^3$, $0.2 < C_{NO_3^-} < 11.5$ $\mu g/m^3$; Asia: $2 < C_{SO_4^{2-}} < 20$ $\mu g/m^3$, $0.7 < C_{NO_3^-} < 20$). References for OC, EC and ion data from other cities are given in Supplemental Table S3.

Figure 1 (c)-(d) illustrate the chemical composition of each $PM_{2.5}$ sample collected during different campaigns of the present study. OM is the dominant component of $PM_{2.5}$ in all campaigns. On average, the main components of these fine particles in each campaign, in decreasing order, are as following:

- Campaign_1, Summer: OM (40.6%), sulfate (18.0%), EC (14.6%), metals (8.6%), ammonium (5.1%), nitrate (0.7%);
- Campaign_1, Winter: OM (42.9%), sulfate (15.4%), EC (13.8%), ammonium (10.5%), metals (4.9%), nitrate (4.3%);
- Campaign_2, Setad: OM (56.0%), sulfate (11.5%), ammonium (9.8%), EC (8.7%), nitrate (4.0%), metals (3.9%).

Ammonium and nitrate concentrations were not quantified for more than half of the samples at the Sharif site in Campaign_2. The correlations of different chemical components between the two sites were investigated. We found slight to no correlation between the two sites for EC (R^2 = 0.39), OC (R^2 = 0.22) and sulfate (R^2 = 0.02). This finding again implies the importance of local sources on forming the bulk chemical composition of $PM_{2.5}$ in Tehran. The low correlation of sulfate between the two sites will be discussed in the PMF analysis section (section 4.2).

3.2. Anthropogenic and crustal elements

Figure 2 shows the concentrations of the measured elements in this study. Also shown are elements enrichment factors (EF), a measure of the extent to which the elements are influenced by anthropogenic sources, calculated as follows:

$$\mathrm{EF} = \frac{\left(C_{\mathrm{X}}/C_{\mathrm{Al}}\right)_{\mathrm{PM}_{2.5}}}{\left(C_{\mathrm{X}}/C_{\mathrm{Al}}\right)_{\text{earth crust}}}. \quad (5)$$

Here, C_X is the concentration of a trace metal X and C_{Al} is the concentration of aluminum. Aluminum is used as reference element as it is expected to be dominated by the suspension of crustal matter. We have used the relative abundances in the earth crust reported by Taylor (1964). EFs close to one indicate crustal origin, whereas higher EFs are an indication of anthropogenic sources. Anthropogenic metals, as suggested by EF values greater than 10 are Ni, V, Mo, Cu, Zn, As, Pb, Cd and Sb, while the crustal elements are Al, Ti, Fe, Rb and Mn. From the mean concentrations of metals, it is evident that elements found in the earth soil make up a large portion of the measured metals (77 ± 17% on average) and soil dust is presumably a contributing source of $PM_{2.5}$ in Tehran.

The most abundant elements were (in decreasing order) Fe (589 ± 448 *ng/m³*), Al (447 ± 382 *ng/m³*), Zn (118 ± 97 *ng/m³*) and Pb (70 ± 62 *ng/m³*). Al and Fe levels in Tehran are higher than those found in Europe and US ($30 < C_{Al} < 160$ *ng/m³*; $50 < C_{Fe} < 400$ *ng/m³*), but lower than in East Asia, South America and the Middle East ($340 < C_{Al} < 2800$ *ng/m³*; $300 < C_{Fe} < 2500$ *ng/m³*). Almost similar trends are observed for anthropogenic elements (Supplemental Figure S6). Their concentrations during winter are higher than in Europe and US and lower than or comparable to those at Asian and South American locations. (e.g. for V, 13 *ng/m³* in Tehran vs. 5.8 *ng/m³* in EU/US and 42 *ng/m³* in Asia/South America; for Cu, 26 *ng/m³* in Tehran vs. 12 *ng/m³* in EU/US and 29 *ng/m³* in Asia/South America; for Zn, 170

ng/m³ in Tehran vs. 36 *ng/m³* in EU/US and 240 *ng/m³* in Asia/South America; for Pb, 121 *ng/m³* in Tehran vs. 31 *ng/m³* in EU/US and 166 *ng/m³* in Asia/South America). References for element concentration data from other cities are given in Supplemental Table S4.

Time series of daily average concentrations of the crustal and non-crustal metals for each campaign are shown in Supplemental Figures S7 and S8. Crustal and anthropogenic elements present very distinct patterns, as suggested by the cluster analysis in Supplemental Figure S9. It is evident that the concentration of crustal elements increases substantially during summer (e.g. C_{Al} = 804 and 303 *ng/m³* during summer and winter, respectively), with stronger winds and drier weather conditions (Figure 2 and Supplemental Figure S7 (a)). By contrast, anthropogenic elements are much more prominent during winter, due to a shallower boundary layer and higher source strengths. A discussion on the boundary layer height effect on seasonal variability of different chemical species is presented in the SI. Amongst the anthropogenic elements, Ni and V represent distinct patterns, as reflected in the cluster analysis (Supplemental Figure S9). In the cold months, thermal power plants in the vicinity of Tehran switch from natural gas to fuel oil which would explain higher levels of V and Ni (C_V = 13.2 and 4.4 *ng/m³*; C_{Ni} = 3.9 and 2.0 *ng/m³* during winter and summer, respectively). Decreased traffic, construction and industrial activities during national holidays can cause lower suspension of dust particles (Figure S7 (b)-(c)), as well as lower emission of anthropogenic metals (Figure S8 (b)-(c)). Average concentrations of all anthropogenic elements in the second campaign are lower than the corresponding winter levels of the first campaign. One should particularly pay attention to the remarkable decrease of the vanadium concentration in the second campaign as a result of stringent monitoring of power plants pollution.

Exploring the correlation between the two sites in the second campaign showed that crustal metals had moderate correlation (e.g. R^2 = 0.46, Setad/Sharif = 1.01 for Al). This is

because dust storms are rather regional. The concentrations of V and Ni correlate well between the two sites, as they originate from a regional source (R^2 = 0.58, Setad/Sharif = 1.02 for Ni and R^2 = 0.46, Setad/Sharif = 1.09 for V). By contrast, other anthropogenic metals exhibited much lower correlations between the two sites (R^2 from 0.05 for Mo to 0.32 for Pb), indicating that the sources of these elements are very local.

3.3. Organic species

Polycyclic Aromatic Hydrocarbons (PAHs): PAHs are formed during incomplete combustion. Average concentrations of 4 to 7-ring PAHs are presented in Supplemental Figure S10 (a). Supplemental Table S5, compares the total PAH concentration in Campaign_2 with the values measured at other urban locations, during cold months. The PAH level in Tehran is close to the lowest values observed in other studies ($1 < C_{PAH} < 260$ *ng/m³*). The correlation between single PAHs is strong (average R^2 of 0.79), indicating a relatively constant fingerprint. Hence, the total PAH concentration was calculated and the time series are plotted in Figure 3 (a). Higher concentrations during the winter inversion period and lower concentrations in summer are evident in the figure (average winter/summer concentration ratio of 2.5). Lower concentrations of PAHs during New Year holidays in the second campaign are also evident, which points towards a reduction in combustion processes. The mean concentration of ∑PAHs was 1.9 *ng/m³* during those holidays, compared to an average of 6.5 *ng/m³* for the rest of the sampling days in Campaign_2.

The concentrations of PAHs at Setad and Sharif sites are very similar (Setad/Sharif = 0.98) and exhibit high correlation, indicating that the emissions of PAHs in Tehran are most likely dominated by regional sources.

Anhydrous sugars: Anhydrous sugars, including galactosan, mannosan and levoglucosan, are markers of biomass combustion, produced upon pyrolysis of cellulose and hemicellulose.

Single anhydrous sugars fairly well correlate with each other (average R^2 of 0.64); thus, their total concentrations are reported in Table 1 and plotted in Figure 3 (b) for both campaigns. Supplemental Figure S10 (b) displays the mean concentrations for the individual sugars. The levoglucosan level in Tehran is lower than the observed values in the Middle East and Europe (Supplemental Table S5). In the areas where wood burning is often used for residential heating, the levoglucosan concentration can exceed 1 $\mu g/m^3$ (e.g. Puxbaum et al., 2007).

Much higher concentrations of levoglucosan were measured during the cold period (average winter/summer concentration of 3.7) and the values reported for Campaign_2 are close to the wintertime concentration of Campaign_1. Biomass burning is not a considerable heating source in Tehran. Therefore, local wood or waste burning in a shallower boundary layer in the cold season and photo-oxidation of levoglucosan in the warm season (Bertrand et al., 2018) could explain the higher concentrations of levoglucosan in winter. The levoglucosan concentration at Setad is half of that at Sharif (Figure 3 (b)) and the correlation of levoglucosan concentrations between the two sites is very weak (R^2 = 0.08), indicating that biomass burning activities in Tehran are not spatially homogeneous.

Normal-alkanes: The carbon preference index (CPI) is a diagnostic parameter for the emission sources of n-alkanes. It is described as the ratio between alkanes with odd carbon number to alkanes with even carbon number:

$$CPI = \frac{\sum C_{2n+1}}{\sum C_{2n}} \quad (6)$$

The n-alkanes originating from vascular plants exhibit high values of CPI, whereas anthropogenic n-alkanes have CPI values close to 1 (Simoneit, 1986). The average CPI value, calculated for n-C_{23} to n-C_{33} alkanes, was 1.14 (0.95–1.26) for the cold days of Campaign_1, 1.51 (1.18–1.82) for the warm days of Campaign_1, 1.03 (0.83–1.37) for Campaign_2 at

Setad site and 1.12 (0.67–1.42) for Campaign_2 at Sharif site. Values very close to unity for all samples suggest a dominant contribution from anthropogenic sources (fossil fuel combustion, gasoline and diesel vehicles exhaust). The distribution of n-alkanes presented in Supplemental Figure S10 (c) is similar to the findings of El Haddad et al. (2009) for PM samples collected in a roadway tunnel in Marseille. High concentrations of the lower molecular weight n-alkanes (< C_{27}) without a clear odd/even predominance pattern found here, are characteristic of tailpipe emissions (Rogge et al., 1993).

The average concentration of n-alkanes in Tehran lies within the range observed in other cities (Supplemental Table S5, 18 < $C_{alkanes}$ < 311 ng/m^3). Concentrations during the cold days of Campaign_1 are close to those of Campaign_2 at both sites, while the ummertime concentrations in Campaign_1 are significantly lower. Alkanes with a lower number of carbon exhibit a higher temperature dependency. For example, the winter/summer concentration ratio of C_{24} is 2.4, while the corresponding ratio for C_{32} is 1.5. This is potentially because of the enhanced partitioning of semi-volatile alkanes at colder temperatures. Despite these differences, individual alkanes are still relatively well correlated (average R^2 of 0.66, see dendrogram based on correlation matrix in Supplemental Figure S11) and exhibit a similar pattern as PAHs and anhydrous sugars (average winter/summer concentration ratio of 1.8).

Figure 3 (c) displays the time series for total n-alkanes measured in this study. Similar to PAHs, the time series of n-alkanes during Campaign_2 does not show any clear trend, except the decrease at the beginning of the New Year holidays. The n-alkanes concentrations are similar at the two sites, but show no correlation, suggesting that these markers derive from local sources.

Hopanes: Hopanes are specific markers of traffic emissions due to their presence in lubrication oil (Schauer et al., 1996). Individual hopanes are highly correlated between each other (an average R^2 value of 0.86), presumably originating from the same sources. Figure 3 (d) displays the times series for the total hopane concentrations at each site during both campaigns. A slight increase is observed during winter inversion episodes. EC/(∑hopanes) obtained in this work (501 ± 272) is close to the lowest values previously found in tunnel studies (1400 ± 900: El Haddad et al., 2009; He et al., 2008). Figure S12 shows the measured levels of EC and total hopanes for all samples and compares them with the measured values near gasoline and diesel-dominated freeways in Los Angeles. Data points are mostly scattered around the line corresponding to the gasoline ratio (Arhami et al., 2009), consistent with the vehicle fleet in Tehran, which is dominated by light-duty passenger cars (72%), mostly running on gasoline, with a minor share of CNG-fueled cars (Shahbazi et al., 2015). As discussed in the following section, samples with EC/(∑hopanes) ratios much lower than the values previously reported for vehicles, are likely influenced by industrial emissions of hopanes.

The average concentration of hopanes in Tehran is close to the highest values reported in other cities (Supplemental Table S5, $0.4 < C_{\text{hopanes}} < 9$ ng/m^3). Individual hopanes in Campaign_2 at Setad site are close to the concentrations of winter days in Campaign_1, but the concentrations at Sharif site in Campaign_2 are all higher. The winter/summer ratio for the total hopanes concentration in Campaign_1 is 1.2, showing little dependency of the hopanes concentration on temperature, opposite to the trends observed for PAHs, anhydrous sugars and n-alkanes. The poor correlation of total hopanes between the two sites in Campaign_2 (R^2 = 0.03) is again attributed to the very local sources of the hopanes, in the same way as the anhydrous sugars and the n-alkanes.

4. Aerosol source apportionment

4.1. Identification of PMF factors

4.1.1 Marker-PMF

The time trends of the five factors resolved by the constrained Marker-PMF are displayed in Figure 4. The relative contributions of each identified factor to the measured variables and their corresponding factor profiles are presented in Supplemental Figure S13.

- Marker Factor 1 – Traffic exhaust

This factor is characterized by high loadings of OC, EC, hopanes and n-alkanes. 75% of OC, 76% of EC and 57% of the hopanes concentration can be explained by this factor. An OC/EC ratio above 2 (2.65) indicates that this factor is largely affected by gasoline vehicles exhaust (Lough et al., 2007), consistent with the vehicle fleet in Tehran as mentioned earlier. The EC/∑hopanes ratio for this factor (743) is also more similar to values reported for gasoline vehicles (450 for gasoline vehicles against 1600 for diesel vehicles, Phuleria et al., 2007). The concentration of this factor in Campaign_1 was generally lower than in Campaign_2 and this accurately reflects the lower concentrations of OC and sum of hopanes in the first campaign (Table 1).

- Marker Factor 2 – Biomass burning

The main organic markers for this factor are anhydrous sugars. 24% of EC and almost half of the observed PAH concentration is apportioned to this factor. The OC/levoglucosan ratio for this factor is 9 which is close to reported values by Shahid et al. (2015) for Pakistani wood species.

- Marker Factor 3 – Industries

Factor 3 is attributed to industrial emission of organic compounds. This factor contributes significantly to PAHs and hopanes, potentially from the combustion of heavy fuel oil (Rogge et al., 1997). The time trends of this factor and the industrial factor resolved from Metal-PMF (see below) are well correlated.

- Marker Factor 4 – Nitrate-rich

This factor is represented by high loadings of NO_3^- and NH_4^+, thus is ascribed to the secondary production of ammonium nitrate aerosol. Higher concentrations of this factor in winter compared to summer are consistent with the semi-volatile nature of ammonium nitrate.

- Marker Factor 5 – Sulfate-rich

The last factor is assigned to secondary ammonium sulfate since 100% of SO_4^{2-} and the remaining NH_4^+ appear in this factor. This factor shows little yearly variability, which agrees with the observed variation in sulfate concentration.

4.1.2 Metal-PMF

The relative contributions and time trends of the four factors resolved by the unconstrained Metal-PMF are illustrated in Figure 5 and their corresponding profiles are presented in the Supplemental Figure S14. Box-and-whiskers plots were created by compiling the results from 20 runs with different initial seeds. The contributions of different factors to different elements are typically consistent across all solutions, except for Cd and As, which can be emitted from a mixture of sources.

- Metal Factor 1 – Dust

The dust factor has the highest loading of Al, Ti, Fe, Mn and Rb, consistent with the enrichment factor analysis (section 3.2). V and Ni have a small contribution to this factor which is consistent with their enrichment factors being close to 10 (Figure 2), indicating mainly anthropogenic sources for these two metals. Another group of metals contributing to this factor consists of Cu, Sb and Mo. These three metals correspond to vehicular emissions and their appearance in the dust factor suggests the influence from re-suspension of road dust. The peak observed in the concentration of this factor during warm months is consistent with the summer dust episode in Tehran, when the wind speed is higher and the relative humidity is the lowest (Supplemental Figure S5). Previous studies in this area have shown that the dust storms originating from the regional dust sources in the Middle East, are frequently observed in the warm seasons (Givehchi et al., 2013; Sowlat et al., 2012).

- Metal Factor 2 – Industries

This factor, attributed to industrial emission of metals, shows loading from anthropogenic heavy metals, such as As, Cd, Pb and Zn. Industrial emissions usually contain various elements since they involve several processes of fossil fuel combustion, mechanical abrasion and metal smelting (Jiang et al., 2018; Kim et al., 2018; Tang et al., 2017). This factor is correlated with the sum of PAHs (R^2 = 0.60) which are also emitted from industrial sources (Figure 4, Marker Factor 3, Industries). As mentioned above, the two industrial factors resolved by two sets of PMF solutions correlate well (R^2 = 0.57).

- Metal Factor 3 – Vehicles (traffic non-exhaust)

This factor is characterized by high loadings of Cu, Sb and Mo. Vehicular emissions are important sources of these metals. Cu is found in tire wear and break abrasion (Lough et al., 2005). Sb is an element of brake lining both in filler and in lubricant (Charron et al., 2019; Gietl et al., 2010). Mo has also been found in brake wear (Dongarra et al., 2009). The factor

profile extracted in Tehran is similar to vehicular wear profiles previously reported at other locations. For example, Visser et al. (2015) reported the presence of Cu, Sb and Mo in the brake wear profile resolved by ME-2, in samples in the size range $PM_{2.5-1.0}$ collected in London. The ratio of Cu/Sb found here (7.7) is in the same range of previously reported ratios for brake wear particles (2.5-10, Pant and Harrison, 2013). It is important to note that leaded gasoline was banned in Iran in 2002, therefore, the contribution of the vehicular factor to Pb is low. Among all factors resolved by Metal-PMF, the Vehicles factor is the best correlated with the sum of hopanes. The concentration of this factor is only slightly enhanced during the winter inversion period, but is decreased during the New Year holidays.

- Metal Factor 4 – Heavy fuel combustion

The fourth factor is dominated by V and Ni. These two elements mostly originate from petrochemical refineries and heavy fuel oil combustion at thermal power plants (Moreno et al., 2010). The V/Ni ratio in this factor (3.5) is consistent with previously reported ratios for fuel oil combustion (El Haddad et al., 2011 and references therein). An abrupt enhancement in the concentration of this factor during the cold season is potentially due to increased consumption of heavy fuel at industrial plants.

4.2. Factor contributions to $PM_{2.5}$

The mean contributions of each of the identified sources to the quantified mass of $PM_{2.5}$ for the yearly campaign of 2014-2015 at Sharif and the first 4 months of 2017 at Sharif and Setad are presented in Figure 6. For each factor, a source specific OM/OC ratio was adopted to convert the apportioned OC to OM concentration, being 1.8 for sulfate- and nitrate-rich factors, 1.2 for primary factors of traffic exhaust and industries and 1.7 for biomass burning factor, resolved from Marker-PMF analysis. The obtained mass weighted average OM/OC was 1.5 which is close to the earlier assumption of 1.4 in Figure 1 (c)-(e). In the pie charts of

Figure 6, industrial factors from Marker- and Metal-PMF were summed up. For comparison, a summary of the previous source apportionment studies in Tehran is also provided in Table 2. It must be emphasized that the contributions reported in Figure 6 are based on the fraction of metals related to each source, that were chemically quantified and the actual source contributions of four factors resolved by Metal-PMF will be higher.

On an annual basis, the major contributor to $PM_{2.5}$ was traffic exhaust, which alone accounted for 42.2% of the total quantified $PM_{2.5}$ mass concentration. Sulfate-rich (33.5%) and nitrate-rich factors (10.1%) were other major contributors. Biomass burning and dust sources had lower contributions (6.1 and 5.8%, respectively). The reported contribution for dust source is only related to the mass of the quantified elements, while dust particles are comprised of metal oxides. In addition, major elements of dust, such as Si, were not measured, which would further increase the dust contribution. To account for oxygen and Si in dust and determine the total crustal matter (CM), we have considered the elements to be present in their common oxide forms of Al_2O_3, SiO_2, Fe_2O_3 and TiO_2 based on the compilation of the data from the IMPROVE network samples in US (Chow et al., 2015):

$$\mathrm{CM} = 1.89\times[\mathrm{Al}] + 1.67\times[\mathrm{Ti}] + 1.87\times[\mathrm{Fe}] + 2.14\times[\mathrm{Si}]. \quad (7)$$

Assuming a Si/Al ratio of 3.41 (Hüglin et al., 2005), the annual average dust concentration would be 5.6 $\mu g/m^3$ (~22% of $PM_{2.5}$) and the average concentration in summer could be as high as 8.4 $\mu g/m^3$ (~32% of $PM_{2.5}$). We note that similar to dust, other metal factors also comprise of unmeasured species; therefore their contributions to $PM_{2.5}$ may be significantly higher than reported here.

The remaining three sources of industries, heavy fuel combustion and traffic non-exhaust had a very little contribution (2.3% in total). Samples in the more recent campaign (2017) at Sharif and Setad sites were collected mostly during winter, thus, larger contributions from the

nitrate-rich and biomass burning factors were obtained. The dust contribution during Campaign_2 was lower than the mean annual value calculated for Campaign_1, since no dust storms took place at that time of the year. Contributions and absolute concentrations of all other minor sources were also consistent between the two sites.

We note that at all sites and campaigns, the traffic exhaust is by far the dominant source of $PM_{2.5}$. This has been previously reported by other studies on $PM_{2.5}$ sources in Tehran as well (Table 2) and conforms to the increasing concern about the massive number of vehicles in this metropolis. Traffic exhaust emissions have constant yearly concentrations, with a slight increase during summer (9.0 $\mu g/m^3$) compared to winter (7.9 $\mu g/m^3$), despite the greater boundary layer height. This may indicate that this factor has some contribution from secondary OC, which could not be separated from primary OC using solely markers of primary emissions, consistent with the increase of $PM_{2.5}$/CO ratio during the day (Figure S4). Still, the traffic exhaust factor is most likely dominated by primary OC, considering the low water solubility of total OC in Tehran (~20% on average). The traffic exhaust contribution to $PM_{2.5}$ in the second campaign was 41.0% (14.2 $\mu g/m^3$) for Sharif and 51.6% (12.5 $\mu g/m^3$) for Setad. This source contributed 56% and 68% to total OM at Sharif and Setad, respectively. This is much higher than the reported values in the US, Europe and China for hydrocarbon-like organic aerosol (HOA). For instance, the HOA contribution to OM was 26% in Las Vegas (Brown et al., 2013), 9.9% in Paris (Petit et al., 2014), 7% in Zurich (Lanz et al., 2010), and 17% in Beijing (Sun et al., 2013).

In summer, sulfate increased due to enhanced photochemical activities, however, its observed seasonality was not considerable, compared to nitrate-rich factor. The contribution of the nitrate-rich factor increased strongly (up to 10 times) during winter. Nitrate-rich factor likely arises from the oxidation of NO_x in traffic and industrial emissions and the subsequent condensation of nitric acid enhanced at lower temperatures. According to the emission

inventory developed for Tehran, fossil fuel combustion in mobile sources and energy conversion sector (power plants and refineries) were responsible for 46.1% and 25% of NO_x emissions, respectively (Shahbazi et al., 2016). The sulfate-rich factor contribution to $PM_{2.5}$ in the second campaign was 12.4% (2.8 $\mu g/m^3$) for Sharif and 21.1% (3.7 $\mu g/m^3$) for Setad. The nitrate-rich factor contribution in the second campaign was 34.2% (14.1 $\mu g/m^3$) for Sharif and 16.1% (3.6 $\mu g/m^3$) for Setad. The major difference between the present results and those of previous CMB and PMF studies in Tehran is the greater share of sulfate- and nitrate-rich factors (secondary aerosol sources) in the present study (40-50%) compared to 18% (CMB, Arhami et al., 2018) and 24-28% (PMF, Taghvaee et al., 2018). The nitrate- and sulfate-rich factors had contributions of 13% and 7.5%, respectively to OC, which can be identified as secondary organic carbon. This adds up to 20.5% which is interestingly in agreement with the average WSOC/OC ratio of 20% measured for both sites and campaigns.

Biomass burning and dust sources also had a strong seasonality. The contribution of the biomass burning factor increased strongly (up to 10 times) during winter and the concentration of the dust factor was almost tripled during summer, making that factor the third major contributor to total quantified $PM_{2.5}$ mass in summer. Other minor sources also experienced a slight enhancement during winter, which is in agreement with the seasonal variability of their specific source markers. The biomass burning contribution in the second campaign was 7.8% (2.2 $\mu g/m^3$) for Sharif and 6.6% (1.6 $\mu g/m^3$) for Setad. Absolute concentrations of other minor sources, in the second campaign, were as follows: total industries (Sharif: 226 ng/m^3, Setad: 132 ng/m^3); heavy fuel combustion (Sharif: 13.6 ng/m^3, Setad: 15.3 ng/m^3); traffic non-exhaust (Sharif: 144 ng/m^3, Setad: 119 ng/m^3). Soil (3-8%) and road dust emissions (< 1%) reported by Taghvaee et al. (2018) are in the same range as the present dust (3-9%) and vehicles non-exhaust emissions (< 1%). However, Taghvaee et

al. (2018) reported higher contributions from biomass burning (16%) and industrial emission (17%).

Figure 7 displays the contributions of the identified sources, distributed across the total daily quantified $PM_{2.5}$ concentration. The WHO guideline of 25 $\mu g/m^3$ was adopted to distinguish the polluted days with a daily limit exceedance of the $PM_{2.5}$ concentration. The highest variability is noticed for the sources with the highest seasonality. On polluted days, the contributions of the nitrate-rich and biomass burning factors increases and that of the sulfate-rich factor decreases, which is not surprising since higher $PM_{2.5}$ concentrations are always recorded in colder months. Traffic exhaust has a consistently high contribution to $PM_{2.5}$ (45%) independent of the total $PM_{2.5}$ concentration.

Exploring the similarities between the time trends of $PM_{2.5}$ sources from site to site helps in recognizing the local or regional behavior of these sources. For this purpose, a correlation analysis was performed between all factors identified at each site and the results are shown in the Supplemental Figure S15. The strongest correlation was observed for the nitrate-rich factor, with $R^2 = 0.9$. Although NO_x emissions are mostly from mobile sources, particle phase nitrate is secondary, formed at a longer time scale and driven by synoptic environmental conditions such as temperature and relative humidity, it is therefore expected to have a more homogeneous spatial distribution. The time trend of the nitrate-rich factor is also well correlated with the ones of biomass burning and heavy fuel combustion, both sources with higher emissions and concentrations in winter.

The second highest correlation was found for the dust factor with an R^2 equal to 0.68, which indicates the spatial homogeneity of this factor, originating from regional dust sources. The next highest correlation was found for the industrial factor resolved by the Metal-PMF solution ($R^2 = 0.64$). This factor along with the heavy fuel combustion factor ($R^2 = 0.58$),

most likely originates from industrial plants located in the western and southern parts of Tehran.

A fairly high correlation between the two sites was observed for the biomass burning factor (R^2 = 0.55), though, with a Setad/Sharif concentration ratio of 0.53. This suggests that, although the type of biomass burnt near each site is different, their temporal trends are similar and there are always higher biomass burning activities during the colder months.

Two factors corresponding to traffic and vehicles showed different behavior. The traffic exhaust factor resolved by Marker-PMF had a weak correlation (R^2 = 0.18) between the two sites, suggesting significant contribution from local rather than regional sources. However, the traffic non-exhaust source identified by the Marker-PMF showed a higher correlation (R^2 = 0.54). This difference can only be explained by the nature of specific markers corresponding to each source. Metals are much less prone to gas-phase chemical reactions compared to OC and this enables them to travel longer distances in the atmosphere while their signature remains the same as they were emitted.

Almost zero correlation for sulfate-rich factor between the two sites is in agreement with the observed correlation for sulfate ion in section 3.1 (R^2 = 0.02). This lack of correlation suggests remarkable contribution from primary sulfate emissions. Substantial SO_2 emission has been reported in Tehran during past years, with an average winter concentration of 30 $\mu g/m^3$ in Campaign_1 and 10 $\mu g/m^3$ in Campaign_2, largely due to the burning of fuels with high sulfur content. The average ratio of $S_{sulfate}/S_{total}$ (sulfur attributed to sulfate to total sulfur in the atmosphere) was 0.1 for the present study. Primary sulfuric acid emissions associated with this magnitude of SO_2 can lead to the absence of correlation between the two sites. The fact that sulfate did not appear in any of the primary sources resolved by the Marker-PMF,

indicates that more data are needed to separate primary from secondary contributions of sulfate in Tehran.

5. Conclusions

A constrained PMF analysis was performed on a comprehensive $PM_{2.5}$ chemical speciation dataset, involving a large number of organic and inorganic markers. Samples were collected during two campaigns at two residential sites in Tehran.

Carbonaceous components (OC and EC) were the major contributors to the quantified fine PM. A large portion of OC in Tehran is water-insoluble, with an average WSOC fraction of 20%. Fossil fuel combustion, especially motor vehicles, are the main primary source of carbonaceous compounds. Sulfate had almost constant concentration during the year while nitrate had a six-time higher concentration during the cold months. Crustal elements had higher concentrations during dust episodes encountered in summer. On the contrary, anthropogenic elements were more enhanced during the cold months.

A total of 9 factors were resolved from the separate PMF analysis of organic compounds (Marker-PMF) and metals (Metal-PMF). Marker-PMF resolved the following factors: Traffic exhaust, biomass burning, industries, sulfate-rich and nitrate-rich. The following factors were resolved from Metal-PMF: Dust, Industries, Vehicles (traffic non-exhaust) and Heavy fuel combustion. Traffic exhaust was the dominant source throughout the year. The mean contributions of traffic exhaust and the secondary factors to OM were 64% and 30%, respectively. This indicates the predominance of primary OA sources over secondary sources. The traffic exhaust and nitrate-rich factors are also the most important sources of $PM_{2.5}$ during polluted days with the $PM_{2.5}$ concentration exceeding the 25 $\mu g/m^3$ limit.

Reasonably high correlations between the two sites were observed for the nitrate-rich, dust, heavy fuel combustion and industrial factors, pointing toward regional sources. Primary sources related to biomass burning and traffic had weaker correlations between the two sites, which suggests significant contributions from local rather than regional sources.

PM is the leading air pollution cause in Tehran. Yet, the prevention strategy seems to be unique and obvious: mitigation strategies should focus on primary PM pollutants of OC and EC, as well as on gaseous precursors of secondary PM (e.g. NO_x, SO_2 and VOCs) which all originate from fossil fuel combustion in mobile and stationary sources.

Acknowledgements

The authors would like to acknowledge the Air Quality Control Company (AQCC) management and staff for granting access to the air monitoring stations, helping with the sampling procedure and providing the required software. We would like to thank Mr. Namdari for his contribution to the field campaigns and Ms Torbatian for providing pollutants and meteorological data. Researchers at Wisconsin State Laboratory of Hygiene would like to thank Brandon Shelton for conducting EC/OC analysis. Jean-Luc Jaffrezo and Gaëlle Uzu would like to thank the LEFE CHAT (program 863353: “Le PO comme proxy de l’impact sanitaire”), and LABEX OSUG@2020 (ANR-10-LABX-56) (both for funding analytical instruments).

Funding: Sepideh Esmaeilirad was funded by Swiss Federal Commission for Scholarships for Foreign Students (FCS).

References

Al-Dabbous, A. N. and Kumar, P., 2015. Source apportionment of airborne nanoparticles in a Middle Eastern city using positive matrix factorization. Environ. Sci.: Processes Impacts, 17, 802–812. https://doi.org/10.1039/c5em00027k.

Alharbi, B., Shareef, M. M., and Husain, T., 2015. Study of chemical characteristics of particulate matter concentrations in Riyadh, Saudi Arabia. Atmos. Pollut. Res., 6, 88–98. https://doi.org/10.5094/APR.2015.011.

Alizadeh-Choobari, O., Bidokhti, A. A., Ghafarian, P., Najafi, M. S., 2016. Temporal and spatial variations of particulate matter and gaseous pollutants in the urban area of Tehran. Atmos. Environ., 141, 443–453. https://doi.org/10.1016/j.atmosenv.2016.07.003.

Alolayan, M. A., Brown, K. W., Evans, J. S., Bouhamra, W. S. and Koutrakis, P., 2013. Source apportionment of fine particles in Kuwait City. Sci. Total Environ., 448, 14–25. https://doi.org/10.1016/j.scitotenv.2012.11.090.

Alves, C., Vicente, A., Pio, C., Kiss, G., Hoffer, A., Decesari, S., Prevot, A. S. H., Minguillon, M. C., Querol, X., Hillamo, R., Spindler, G. and Swietlicki, E., 2012. Organic compounds in aerosols from selected European sites- Biogenic versus anthropogenic sources. Atmos. Environ., 59, 243–255. https://doi.org/10.1016/j.atmosenv.2012.06.013.

Arhami, M., Hosseini, V., Zare Shahne, M., Bigdeli, M., Lai, A. M. and Schauer, J. J., 2017. Seasonal trends, chemical speciation and source apportionment of fine PM in Tehran. Atmos. Environ., 153, 70–82. https://doi.org/10.1016/j.atmosenv.2016.12.046.

Arhami M., Sillanpaa M., Hu S., Olson M. R., Schauer J. J., and Sioutas C., 2009. Size-segregated inorganic and organic components of PM in the communities of the Los Angeles harbor. Aerosol Sci. Technol., 43, 145–160. https://doi.org/10.1080/02786820802534757.

Arhami, M., Zare Shahne, M., Hosseini, V., Roufigar Haghighat, N., Lai, A. M. and Schauer, J. J, 2018. Seasonal trends in the composition and sources of $PM_{2.5}$ and carbonaceous aerosol in Tehran, Iran. Environ. Pollut., 239, 69–81. https://doi.org/10.1016/j.envpol.2018.03.111.

Bae, M., Skiles, M. J., Lai, A. M., Olson, M. R., de Foy, B. and Schauer, J. J., 2019. Assessment of forest fire impacts on carbonaceous aerosols using complementary molecular marker receptor models at two urban locations in California's San Joaquin Valley. Environ. Pollut., 246, 274–283. https://doi.org/10.1016/j.envpol.2018.12.013.

Bertrand, A., Stefenelli, G., Jen, C. N., Pieber, S. M., Bruns, E. A., Ni, H., Temime-Roussel, B., Slowik, J. G., Goldstein, A. H., El Haddad, I., Baltensperger, U., Prévôt, A. S. H., Wortham, H., and Marchand, N., 2018. Evolution of the chemical fingerprint of biomass burning organic aerosol during aging, Atmos. Chem. Phys., 18, 7607–7624. https://doi.org/10.5194/acp-18-7607-2018.

Bian, Q., Alharbi, B., Shareef, M. M., Husain, T., Pasha, M. J., Atwood, S. A., and Kreidenweis, S. M., 2018. Sources of $PM_{2.5}$ carbonaceous aerosol in Riyadh, Saudi Arabia. Atmos. Chem. Phys., 18, 3969–3985. https://doi.org/10.5194/acp-18-3969-2018.

Birch, M. and Cary, R., 1996. Elemental carbon-based method for monitoring occupational exposures to particulate diesel exhaust. Aerosol Sci. Tech., 25, 221–241. https://doi.org/10.1080/02786829608965393.

Bozzetti, C., Sosedova, Y., Xiao, M., Daellenbach, K. R., Ulevicius, V., Dudoitis, V., Mordas, G., Byčenkienė, S., Plauškaitė, K., Vlachou, A., Golly, B., Chazeau, B., Besombes, J. -L., Baltensperger, U., Jaffrezo, J.-L., Slowik, J. G., El Haddad, I. and Prévôt, A. S. H., 2017. Argon offline-AMS source apportionment of organic aerosol over

yearly cycles for an urban, rural, and marine site in northern Europe. Atmos. Chem. Phys., 17, 117–141. https://doi.org/10.5194/acp-17-117-2017.

Brown, S. G., Lee, T., Roberts, P. T. and Collette, J. L., 2013. Variations in the OM/OC ratio of urban organic aerosol next to a major roadway. J. Air Waste Manage. Assoc., 63, 1422–1433. https:\\doi.org\10.1080/10962247.2013.826602.

Callén, M. S., Iturmendi, A. and López, J. M., 2014. Source apportionment of atmospheric $PM_{2.5}$-bound polycyclic aromatic hydrocarbons by a PMF receptor model. Assessment of potential risk for human health. Environ., Pollut., 195, 167–177. https://doi.org/10.1016/j.envpol.2014.08.025.

Canonaco, F., Crippa, M., Slowik, J. G., Baltensperger, U., and Prévôt, A. S. H., 2013. SoFi, an IGOR-based interface for the efficient use of the generalized multilinear engine (ME-2) for the source apportionment: ME-2 application to aerosol mass spectrometer data. Atmos. Meas. Tech., 6, 3649–3661. https://doi.org/10.5194/amt-6-3649-2013.

Cass, G. R., 1998. Organic molecular tracers for particulate air pollution sources. Trac. Trends. Anal. Chem., 17, 356–366. https://doi.org/10.1016/S0165-9936(98)00040-5.

Charron, A., Polo-Rehn, L., Besombes, J.-L., Golly, B., Buisson, C., Chanut, H., Marchand, N., Guillaud, G. and Jaffrezo, J.-L., 2019. Identification and quantification of particulate tracers of exhaust and non-exhaust vehicle emissions. Atmos. Chem. Phys., 19, 5187–5207. https://doi.org/10.5194/acp-19-5187-2019.

Chow, J. C., Lowenthal, D. H., Chen, L. W. A., Wang, X. and Watson, J. G., 2015. Mass reconstruction methods for $PM_{2.5}$: a review. Air Qual. Atmos. Health, 8, 243–263. https://doi.org/10.1007/s11869-015-0338-3.

Cohen, A. J., Brauer, M., Burnett, R., Anderson, H. R., Frostad, J., Estep, K., Balakrishnan, K., Brunekreef, B., Dandona, L., Dandona, R., Feigin, V., Freedman, G., Hubbell, B.,

Jobling, A., Kan, H., Knibbs, L., Liu, Y., Martin, R., Morawska, L., Pope III, C. A., Shin, H., Straif, K., Shaddick, G., Thomas, M., Dingenen, R., van Donkelaar, A., Vos, T., Murray, C. J. L. and Forouzanfar, M. H., 2017. Estimates and 25-year trends of the global burden of disease attributable to ambient air pollution: an analysis of data from the Global Burden of Diseases Study 2015. Lancet, 389, 1907–1918. https://doi.org/10.1016/ S0140-6736(17)30505-6.

Daellenbach, K. R., Bozzetti, C., Křepelová, A., Canonaco, F., Wolf, R., Zotter, P., Fermo, P., Crippa, M., Slowik, J. G., Sosedova, Y., Zhang, Y., Huang, R.-J., Poulain, L., Szidat, S., Baltensperger, U., El Haddad, I., and Prévôt, A. S. H., Characterization and source apportionment of organic aerosol using offline aerosol mass spectrometry. Atmos. Meas. Tech., 9, 23–39. https://doi.org/10.5194/amt-9-23-2016.

Decesari, S., Facchini, M., Fuzzi, S., McFiggans, G., Coe, H. and Bower, K., 2005. The water-soluble organic component of size-segregated aerosol, cloud water and wet depositions from Jeju Island during ACE-Asia. Atmos. Environ., 39, 211–222. https://doi.org/10.1016/j.atmosenv.2004.09.049.

Dongarra, G., Manno, E. and Varrica, D., 2009. Possible markers of traffic-related emissions. Environ. Monit. Assess., 154, 117–125. https://doi.org/10.1007/s10661-008-0382-7.

Dutton, S. J., Vedal, S., Piedrahita, R., Milford, J. B., Miller, S. L. and Hannigan, M. P., 2010. Source apportionment using positive matrix factorization on daily measurements of inorganic and organic speciated $PM_{2.5}$. Atmos. Environ., 44, 2731–2741. https:// doi.org/10.1016/j.atmosenv.2010.04.038.

El Haddad, I., Marchand, N., Dron, J., Temime-Roussel, B., Quivet, E., Wortham, H., Jaffrezo, J.-L., Baduel, C., Voisin, D., Besombes, J. L. and Gille, G., 2009. Comprehensive primary particulate organic characterization of vehicular exhaust

emissions in France. Atmos. Environ., 43, 6190–6198. https://doi.org/10.1016/j.atmosenv.2009.09.001.

El Haddad, I., Marchand, N., Wortham, H., Piot, C., Besombes, J.-L., Cozic, J., Chauvel, C., Armengaud, A., Robin, D. and Jaffrezo, J.-L., 2011. Primary sources of $PM_{2.5}$ organic aerosol in an industrial Mediterranean city, Marseille, Atmos. Chem. Phys., 11, 2039–2058, https://doi.org/10.5194/acp-11-2039-2011.

Engelbrecht J. P. and Jayanty R., 2013. Assessing sources of airborne mineral dust and other aerosols, in Iraq. Aeolian Res., 9, 153–160. https://doi.org/10.1016/j.aeolia.2013.02.003.

Gietl, J. K., Lawrence, R., Thorpe, A. J. and Harrison, R. M., 2010. Identification of brake wear particles and derivation of a quantitative tracer for brake dust at a major road. Atmos. Environ., 44, 141–146. https://doi.org/10.1016/j.atmosenv.2009.10.016.

Givehchi, R., Arhami, M., Tajrishy, M., 2013. Contribution of the Middle Eastern dust source areas to PM_{10} levels in urban receptors: case study of Tehran, Iran. Atmos. Environ. 75, 287–295. https://doi.org/10.1016/j.atmosenv.2013.04.039.

Gupta, S., Gadi, R., Sharma, S. K. and Mandal, T. K., 2018. Characterization and source apportionment of organic compounds in PM_{10} using PCA and PMF at a traffic hotspot of Delhi. Sustain. Cities Soc., 39, 52–67. https://doi.org/10.1016/j.scs.2018.01.051.

Habre, R., Moshier, E., Castro, W., Nath, A., Grunin, A., Rohr, A., Godbold, J., Schachter, N., Kattan, M. and Coull, B., 2014. The effects of $PM_{2.5}$ and its components from indoor and outdoor sources on cough and wheeze symptoms in asthmatic children. J. Expo. Sci. Env. Epidemiol., 24, 380–387. https://doi.org/10.1038/jes.2014.21.

Hallquist, M., Wenger, J., Baltensperger, U., Rudich, Y., Simpson, D., Claeys, M., Dommen, J., Donahue, N., George, C., Goldstein, A., 2009. The formation, properties and impact of

secondary organic aerosol: current and emerging issues. Atmos. Chem. Phys., 9, 5155–5236. https://doi.org/10.5194/acp-9-5155-2009.

Hamad, S. H., Schauer, J. J., Heo, J. and Kadhim, A. K., 2015. Source apportionment of $PM_{2.5}$ carbonaceous aerosol in Baghdad, Iraq. Atmos. Res., 156, 80–90. https://doi.org/10.1016/j.atmosres.2014.12.017.

Harrison, R. M., Jones, A. M., Gietl, J., Yin, J. and Green, D. C., 2012. Estimation of the contributions of brake dust, tire wear, and resuspension to non-exhaust traffic particles derived from atmospheric measurements. Environ. Sci. Technol., 46, 6523–6529. https://doi.org/10.1021/es300894r.

He, L.-Y., Hu, M., Zhang, Y.-H., Huang, X.-F., and Yao, T.-T., 2008. Fine particle emissions from on-road vehicles in the Zhujiang tunnel, China. Environ. Sci. Technol., 42, 4461–4466. https://doi.org/10.1021/es7022658.

HEI, HEI perspectives 3, 2013. Understanding the health effects of ambient ultrafine particles (HEI review panel on ultrafine particles). Health Effects Institute, Boston, Massachusetts. https://www.healtheffects.org/system/files/Perspectives3.pdf.

Heo, J., Dulger, M., Olson, M. R., McGinnis, J. E., Shelton, B. R., Matsunaga, A., Sioutas, C. and Schauer, J. J., 2013. Source apportionments of $PM_{2.5}$ organic carbon using molecular marker positive matrix factorization and comparison of results from different receptor models. Atmos. Environ., 73, 51–61. https://doi.org/10.1016/j.atmosenv.

Heo, J., Wu, B., Abdeen, Z., Qasrawi, R., Sarnat, J. A., Sharf, G., Shpund, K. and Schauer, J. J., 2017. Source apportionments of ambient fine particulate matter in Israeli, Jordanian, and Palestinian cities. Environ. Pollut., 225, 1–11. https://doi.org/10.1016/j.envpol.2017.01.081.

Hidy, G., 1994. Atmospheric sulfur and nitrogen oxides: Eastern North American source-receptor relationships, vol. 60.

Hosseini, V. and Shahbazi, H., 2016. Urban air pollution in Iran. Iran. Stud. 49 (6), 1029–1046. http://doi.org/10.1080/00210862.2016.1241587.

Huang, R.-J., Wang, Y., Cao, J., Lin, C., Duan, J., Chen, Q., Li, Y., Gu, Y., Yan, J., Xu, W., Fröhlich, R., Canonaco, F., Bozzetti, C., Ovadnevaite, J., Ceburnis, D., Canagaratna, M. R., Jayne, J., Worsnop, D. R., El Haddad, I., Prévôt, A. S. H., and O'Dowd, C. D., 2019. Primary emissions versus secondary formation of fine particulate matter in the most polluted city (Shijiazhuang) in North China. Atmos. Chem. Phys., 19, 2283–2298, https://doi.org/10.5194/acp-19-2283-2019.

Hüglin, C., Gehrig, R., Baltensperger, U., Gysel, M., Monn, C. and Vonmont, H., 2005. Chemical characterization of $PM_{2.5}$, PM_{10} and coarse particles at urban, near-city and rural sites in Switzerland. Atmos. Environ. 39, 637–651. https://doi.org/10.1016/j.atmosenv.2004.10.027.

Jaafari, J., Naddafi, K., Yunesian, M., Nabizadeh, R., Hassanvand, M., S., Ghanbari Ghozikali, M., Nazmara, S., Shamsollahi, H. R., and Yaghmaeian, K., 2017. Study of PM_{10}, $PM_{2.5}$ and PM_1 levels in during dust storms and local air pollution events in urban and rural sites in Tehran, Hum. Ecol. Risk. Assess., 24(2), 482–493. https://doi.org/10.1080/10807039.2017.1389608.

Jiang, N., Yin. S., Guo, Y., Li, J., Kang, P., Zhang, R. and Tang, X., 2018. Characteristics of mass concentration, chemical composition, source apportionment of $PM_{2.5}$ and PM_{10} and health risk assessment in the emerging megacity in China. Atmos. Pollut. Res., 9, 309–321. https://doi.org/10.1016/j.apr.2017.07.005.

Jimenez, J. L., Canagaratna, M. R., Donahue, N. M., Prevot, A. S. H., Zhang, Q., Kroll, J. H., DeCarlo, P. F., Allan, J. D., Coe, H., Ng, N. L., Aiken, A. C., Docherty, K. D., Ulbrich, I. M., Grieshop, A. P., Robinson, A. L., Duplissy, J., Smith, J. D., Wilson, K. R., Lanz, V. A., Hüglin, C., Sun, Y. L., Tian, J., Laaksonen, A., Raatikainen, T., Rautiainen, J., Vaattovaara, P., Ehn, M., Kulmala, M., Tomlinson, J. M., Collins, D. R., Cubison, M. J., Dunlea, E. J., Huffman, J. A., Onasch, T. B., Alfarra, M. R., Williams, P. I., Bower, K., Kondo, Y., Schneider, J., Drewnick, F., Borrmann, S., Weimer, S., Demerjian, K., Salcedo, D., Cottrell, L., Griffin, R., Takami, A., Miyoshi, T., Hatakeyama, S., Shimono, A., Sun, J. Y, Zhang, Y. M., Dzepina, K., Kimmel, J. R., Sueper, D., Jayne, J. T., Herndon, S. C., Trimborn, A. M., Williams, L. R., Wood, E. C., Kolb, C. E., Middlebrook, A. M., Baltensperger, U., and Worsnop, D. R., 2009. Evolution of organic aerosols in the atmosphere. Science, 326, 1525. https://doi.org/10.1126/science.1180353.

Khodeir, M., Shamy, M., Alghamdi, M., Zhong, M., Sun, H., Costa, M., Chen, L.-C. and Maciejczyk, P., 2012. Source apportionment and elemental composition of $PM_{2.5}$ and PM_{10} in Jeddah City, Saudi Arabia. Atmos. Pollut. Res., 3, 331–340. https://doi.org/10.5094/APR.2012.037.

Kim, S., Kim, T. Y., Yi, S. M. and Heo, J., 2018. Source apportionment of $PM_{2.5}$ using positive matrix factorization (PMF) at a rural site in Korea. J. Environ. Manage., 214, 325–334. https://doi.org/10.1016/j.jenvman.2018.03.027.

Koçaka, M., Theodosi, C., Zarmpas, P., Im, U., Bougiatioti, A., Yenigun, O. and Mihalopoulos, N., 2011. Particulate matter (PM_{10}) in Istanbul: Origin, source areas and potential impact on surrounding regions. Atmos. Environ., 45, 6891–6900. https://doi.org/10.1016/j.atmosenv.2010.10.007.

Koton, S., Molshatzki, N., Myers, V., Broday, D. M., Drory, Y., Steinberg, D. M. and Gerber, Y., 2013. Cumulative exposure to particulate matter air pollution and long-term post-myocardial infarction outcomes. Prev. Med., 57, 339–344. https://doi.org/10.1016/j.ypmed.2013.06.009.

Lanz, V. A., Prévôt, A. S. H., Alfarra, M. R., Weimer, S., Mohr, C., DeCarlo, P. F., Gianini, M. F. D., Hüglin, C., Schneider, J., Favez, O., D'Anna, B., George, C. and Baltensperger, U., 2010. Characterization of aerosol chemical composition with aerosol mass spectrometry in Central Europe: an overview. Atmos. Cüem. Phys., 10, 10453–10471. https://doi.org/10.5194/acp-10-10453-2010.

Lough G. C., Christensen C. G., Schauer J. J., Tortorelli J., Mani E., Lawson D. R., Clark N. N. and Gabele P. A., 2007. Development of molecular marker source profiles for emissions from on-road gasoline and diesel vehicle fleets. J. Air Waste Manage. Assoc., 57, 1190–1199. https://doi.org/10.3155/1047-3289.57.10.1190.

Lough, G. C., Schauer, J. J., Park, J.-S., Shafer, M. M., DeMinter, J. T. and Weinstein, J. P., 2005. Emissions of metals associated with motor vehicle roadways. Environ. Sci. Technol., 39, 826–836. https://doi.org/10.1021/es048715f.

Mohseni Bandpi, A., Eslami, A., Shahsavani, A., Khodagholi, F. and Alinejad, A., 2017. Physicochemical characterization of ambient $PM_{2.5}$ in Tehran air and its potential cytotoxicity in human lung epithelial cells (A549). Sci. Total Environ., 593-594, 182–190. https://doi.org/10.1016/j.scitotenv.2017.03.150.

Moreno, T., Querol, X., Alastuey, A., de la Rosa, J., Sánchez de la Campa, A. M., Minguillón, M., Pandolfi, M., González-Castanedo, Y., Monfort, E. and Gibbons, W., 2010. Variations in vanadium, nickel and lanthanoid element concentrations in urban air. Sci. Total Environ., 408, 4569–4579. https://doi.org/10.1016/j.scitotenv.2010.06.016.

Nayebare, S. R., Aburizaiza, O. S., Khwaja, H. A., Siddique, A., Hussain, M. M., Zeb, J., Khatib, F., Carpenter, D. O. and Blake, D. R., 2016. Chemical characterization and source apportionment of $PM_{2.5}$ in Rabigh, Saudi Arabia. Aerosol Air Qual. Res., 16, 3114–3129. https:// doi.org/10.4209/aaqr.2015.11.0658.

Nayebare S. R., Aburizaiza, O. S., Siddique, A., Carpenter, D. O., Hussain, M. M, Zeb, J., Aburiziza A. J. and Khwaja, H. A., 2018. Ambient air quality in the holy city of Makkah: A source apportionment with elemental enrichment factors (EFs) and factor analysis (PMF). Environ. Pollut., Part B, 243, 1791–1801. https://doi.org/10.1016/j.envpol.2018.09.086.

Orasche, J., Schnelle-Kreis, J., Abbaszade, G., and Zimmermann, R., 2011. Technical note: in-situ derivatization thermal desorption GC-TOFMS for direct analysis of particle-bound non-polar and polar organic species. Atmos. Chem. Phys., 11, 8977–8993. https://doi.org/10.5194/acp-11-8977-2011.

Paatero, P., 1999. The multilinear engine – A table-driven, least squares program for solving multilinear problems, including the n-way parallel factor analysis model. J. Comput. Graph. Stat., 8, 854–888. https://doi.org/10.1080/10618600.1999.10474853.

Paatero, P. and Hopke, P. K., 2003. Discarding or downweighting high-noise variables in factor analytic models. Anal. Chim. Acta, 490, 277–289. https://doi.org/10.1016/s0003-2670(02)01643-4.

Paatero, P. and Tapper, U., 1994. Positive matrix factorization: a non-negative factor model with optimal utilization of error estimates of data values. Environ. Metrics., 5, 111–126. https://doi.org/10.1002/env.3170050203.

Paatero, P., Hopke, P. K., Song, X. H. and Ramadan, Z., 2002. Understanding and controlling rotations in factor analytic models. Chemom. Intell. Lab. Syst., 60, 253–264. https://doi.org/10.1016/s0169-7439(01)00200-3.

Pant P. and Harrison R. M., 2013. Estimation of the contribution of road traffic emissions to particulate matter concentrations from field measurements: A review. Atmos. Environ., 77, 78–97. http://dx.doi.org/10.1016/j.atmosenv.2013.04.028.

Pateraki, S., Manousakas, M., Bairachtari, K., Kantarelou, V., Eleftheriadis, K., Vasilakos, C., Assimakopoulos, V. D. and Maggos, T., 2019. The traffic signature on the vertical PM profile: Environmental and health risks within an urban roadside environment. Sci. Total Environ., 646, 448–459. https://doi.org/10.1016/j.scitotenv.2018.07.289.

Peltier, R. E. and Lippmann, M., 2010. Residual oil combustion: 2. Distributions of airborne nickel and vanadium within New York City. J. Expo. Sci. Env. Epid., 20, 342–50, https://doi.org/10.1038/jes.2009.28, 2010.

Petit, J.-E., Favez, O., Sciare, J., Canonaco, F., Croteau, P., Močnik, G., Jayne, J., Worsnop, D. and Leoz-Garziandia, E., 2014. Submicron aerosol source apportionment of wintertime pollution in Paris, France by double positive matrix factorization (PMF) using an aerosol chemical speciation monitor (ACSM) and a multi-wavelength Aethalometer. Atmos. Chem. Phys., 14, 13773–13787. https://doi.org/10.5194/acp-14-13773-2014.

Phuleria, H. C., Sheesley, R. J., Schauer, J. J., Fine, P. M., and Sioutas, C., 2007. Roadside measurements of size-segregated particulate organic compounds near gasoline and diesel-dominated freeways in Los Angeles, CA, Atmos. Environ., 41, 4653–4671. https://doi.org/10.1016/j.atmosenv.2007.03.031.

Puxbaum, H., Caseiro, A., Sánchez-Ochoa, A., Kasper-Giebl, A., Claeys, M., Gelencsér, A., Legrand, M., Preunkert, S. and Pio, C., 2007. Levoglucosan levels at background sites in

Europe for assessing the impact of biomass combustion on the European aerosols background. J. Geophys. Res., 112, D23S05. http://dx.doi.org/10.1023/2006JD008114.

Querol, X., Viana, M., Alastuey, A., Amato, F., Moreno, T., Castillo, S., Pey, J., de la Rosa, J., Sánchez de la Campa, A., Artiñano, B., Salvador, P., García dos Santos, S., Fernández-Patier, R., Moreno-Grau, S., Negral, L., Minguillón, M. C., Monfort, E., Gil, J. I., Inza, A., Ortega, L. A., Santamaría, J. M. and Zabalza, J., 2007. Source origin of trace elements in PM from regional background, urban and industrial sites of Spain. Atmos. Environ., 41, 7219–7231. https://doi.org/10.1016/j.atmosenv.2007.05.022.

Rocke, D. M. and Lorenzato, S., 1995. A two-component model for measurement error in analytical chemistry, Technometrics, 37, 176– 184. https://doi.org/10.1080/00401706.1995.10484302.

Rogge, W. F., Hildemann, L. M., Mazurek, M. A., Cass, G. R., Simoneit, B. R. T., 1993. Sources of fine organic aerosol. 2. Noncatalyst and catalyst-equipped automobiles and heavy-duty diesel trucks. Environ. Sci. Technol., 27, 636 – 651. https://doi.org/10.1021/es00041a007.

Rogge, W. F., Hildemann, L. M., Mazurek, M. A., Cass, G. R., Simoneit, B. R. T., 1997. Sources of fine organic aerosol. 8. Boilers burning no. 2 distillate fuel oil. Environ. Sci. Technol., 31, 2731–2737. http://dx.doi.org/10.1021/es9609563.

Salameh, D., Pey, J., Bozzetti, C., El Haddad, I., Detournay, A., Sylvestre, A., Canonaco, F., Armengaud, A., Piga, D., Robin, D., Prevot, A. S. H., Jaffrezo, J.-L, Wortham, H. and Marchand, N., 2018. Sources of $PM_{2.5}$ at an urban-industrial Mediterranean city, Marseille (France): Application of the ME-2 solver to inorganic and organic markers. Atmos. Res., 214, 263–274. https://doi.org/10.1016/j.atmosres.2018.08.005.

Samaké, A., Jaffrezo, J. L., Favez, O., Weber, S., Jacob, V., Albinet, A., Riffault, V., Perdrix, E., Waked, A., Golly, B., Salameh, D., Chevrier, F., Oliveira, D., Bonnaire, N., Besombes, J. L., Martins, J. M. F., Conil, S., Guillaud, G., Mesbah, B., Rocq, B., Robic, P. Y., Hulin, A., Le Meur, S., Descheemaecker, M., Chretien, E., Marchand, N. and Uzu, G., 2019. Polyols and glucose particulate species as tracers of primary biogenic organic aerosols at 28 French sites. Atmos. Chem. Phys., 19, 3357–3374. https://doi.org/10.5194/acp-19-3357-2019.

Schauer, J. J., Mader, B., Deminter, J., Heidemann, G., Bae, M., Seinfeld, J. H., Flagan, R., Cary, R., Smith, D. and Huebert, B., 2003. ACE-Asia inter-comparison of a thermal optical method for the determination of particle-phase organic and elemental carbon. Environ. Sci. Technol., 37, 993–1001. https://doi.org/10.1021/es020622f.

Schauer, J. J., Rogge, W. F., Hildemann, L. M., Mazurek, M. A., Cass, G. R. and Simoneit, B. R., 1996. Source apportionment of airborne particulate matter using organic compounds as tracers. Atmos. Environ., 30, 3837–3855. https://doi.org/10.1016/1352-2310(96)00085-4.

Shahbazi, H., Reyhanian, M., Hosseini, V., Afshin, H., 2015. The relative contributions of mobile sources to air pollutant emissions in Tehran, Iran: an emission inventory approach. J. Emiss. Control Sci. Technol., 2, 44–56. https://doi.org/10.1007/s40825-015-0031-x.

Shahbazi, H., Taghvaee, S., Hosseini, V. and Afshin, H., 2016. A GIS based emission inventory development for Tehran. Urban Clim., 17, 216–229. https://doi.org/10.1016/j.uclim.2016.08.005.

Shahid, I., Kistler, M., Mukhtar, A., Ramirez-Santa Cruz, C., Bauer, H. and Puxbaum, H., 2015. Chemical composition of particles from traditional burning of Pakistani wood species. Atmos. Environ., 121, 35–41. https://doi.org/10.1016/j.atmosenv.2015.01.041.

Simoneit, B. R. T., 1986. Characterization of organic-constituents in aerosols in relation to their origin and transports: A review. Int. J. Environ. Anal.Chem., 23, 207–237.

Simoneit, B. R. T, Schauer, J. J., Nolte, C., Oros, D. R., Elias, V. O., Fraser, M., Rogge, W., Cass, G. R., 1999. Levoglucosan, a tracer for cellulose in biomass burning and atmospheric particles. Atmos. Environ., 33, 173–182. https://doi.org/10.1016/S1352-2310(98)00145-9.

Sowlat, M. H., Naddafi, K., Yunesian, M., Jackson, P. L., Shahsavani, A., 2012. Source apportionment of total suspended particulates in an arid area in southwestern Iran using Positive Matrix Factorization. Bull. Environ. Contam. Toxicol., 88, 735–740. https://doi.org 10.1007/s00128-012-0560-8.

Sun, Y. L., Wang, Z. F., Fu, P. Q., Yang, T., Jiang, Q., Dong, H. B., Li, J., and Jia, J. J., 2013. Aerosol composition, sources and processes during wintertime in Beijing, China. Atmos. Chem. Phys., 13, 4577–4592. https://doi.org/10.5194/acp-13-4577-2013.

Taghvaee, S., Sowlat, M. H., Mousavi, A., Hassanvand, M. S., Yunesian, M., Naddafi, K. and Sioutas, C., 2018. Source apportionment of ambient $PM_{2.5}$ in two locations in central Tehran using the positive matrix factorization (PMF) model. Sci. Total Environ., 628-629, 672–686. https://doi.org/10.1016/j.scitotenv.2018.02.096.

Tang, X., Chen, X. and Tian, Y., 2017. Chemical composition and source apportionment of $PM_{2.5}$ - A case study from one year continuous sampling in the Chang-Zhu-Tan urban agglomeration. Atmos. Pollut. Res., 8, 885–899. http://doi.org/10.1016/j.apr.2017.02.004.

Taylor, S. R., 1964. Abundance of chemical elements in the continental crust: a new table. Geochimica et Cosmochimica Acta, 28, 1273–1285. https://doi.org/10.1016/0016-7037(64)90129-2.

Tecer, L. H., Tuncel, G., Karaca, F., Alagha, O., Süren, P., Zararsiz, A. and Kirmaz, R., 2012. Metallic composition and source apportionment of fine and coarse particles using positive matrix factorization in the southern Black Sea atmosphere. Atmos. Res., 118, 153–169. https://doi.org/10.1016/j.atmosres.2012.06.016.

Turpin, B. J. and Lim, H. J., 2001. Species Contributions to $PM_{2.5}$ mass concentrations: Revisiting common assumptions for estimating organic mass. Aerosol Sci. Technol., 35, 602–610.

Van Ryswyk, K., Wheeler, A. J., Wallace, L., Kearney, J., You, H., Kulka, R. and Xu, X., 2014. Impact of microenvironments and personal activities on personal $PM_{2.5}$ exposures among asthmatic children. J. Expo. Sci. Env. Epidemiol., 24, 260. https://doi.org/10.1038/jes.2013.20.

Villalobos, A. M., Barraza, F., Jorquera, H. and Schauer, J. J., 2015. Chemical speciation and source apportionment of fine particulate matter in Santiago, Chile, 2013. Sci. Total Environ., 512, 133–142. https://doi.org/10.1016/j.scitotenv.2015.01.006.

Visser, S., Slowik, J. G., Furger, M., Zotter, P., Bukowiecki, N., Canonaco, F., Flechsig, U., Appel, K., Green, D. C., Tremper, A. H., Young, D. E., Williams, P. I., Allan, J. D., Coe, H., Williams, L. R., Mohr, C., Xu, L., Ng, N. L., Nemitz, E., Barlow, J. F., Halios, C. H., Fleming, Z. L., Baltensperger, U. and Prévôt, A. S. H., 2015. Advanced source apportionment of size-resolved trace elements at multiple sites in London during winter. Atmos. Chem. Phys., 15, 11291–11309. https://doi.org/10.5194/acp-15-11291-2015.

Vlachou, A., Daellenbach, K. R., Bozzetti, C., Chazeau, B., Salazar, G. A., Szidat, S., Jaffrezo, J.-L., Hüglin, C., Baltensperger, U., Haddad, I. E., and Prévôt, A. S. H., 2018. Advanced source apportionment of carbonaceous aerosols by coupling offline AMS and

radiocarbon size-segregated measurements over a nearly 2-year period. Atmos. Chem. Phys., 18, 6187–6206. https://doi.org/10.5194/acp-18-6187-2018.

von Schneidemesser, E., Zhou, J., Stone, E. A., Schauer, J. J., Qasrawi, R., Abdeen, Z., Shpund, J., Vanger, A., Sharf, G., Moise, T., Brenner, S., Nassar, K., Saleh, R., Al-Mahasneh, Q. M. and Sarnat, J. A., 2010. Seasonal and spatial trends in the sources of fine particle organic carbon in Israel, Jordan, and Palestine. Atmos. Environ., 44, 3669–3678. https://doi.org/10.1016/j.atmosenv.2010.06.039.

Vossler, T., Černikovský, L., Novák, J. and Williams, R., 2016. Source apportionment with uncertainty estimates of fine particulate matter in Ostrava, Czech Republic using positive matrix factorization. Atmos. Pollut. Res., 7(3), 503–512. https://doi.org/10.1016/j.apr.2015.12.004.

Waked, A., Afif, C., Brioude, J., Formenti, P., Chevaillier, S., El Haddad, I., Doussin, J. F., Borbon, A. and Seigneur, C., 2013. Composition and source apportionment of organic aerosol in Beirut, Lebanon, during winter 2012. Aerosol Sci. Technol., 47, 1258–1266. https://doi.org/10.1080/02786826.2013.831975.

Waked, A., Favez, O., Alleman, L. Y., Piot, C., Petit, J. E., Delaunay, T., Verlinden, E., Golly, B., Besombes, J. L., Jaffrezo, J.-L. and Leoz-Garziandia, E., 2014. Source apportionment of PM_{10} in a north-western Europe regional urban background site (Lens, France) using positive matrix factorization and including primary biogenic emissions. Atmos. Chem. Phys., 14, 3325–3346. https://doi.org/10.5194/acp-14-3325-2014.

Wang, J. Z., Ho, S. S. H., Cao, J. J., Huang, R. J., Zhou, J. M., Zhao, Y. Z., Xu, H. M., Liu, S. X., Wang, G. H., Shen, Z. X. and Han, Y. M., 2015. Characteristics and major sources of carbonaceous aerosols in $PM_{2.5}$ from Sanya, China. Sci. Total Environ., 530, 110–119. https://doi.org/10.1016/j.scitotenv.2015.05.005.

WHO, 2016, Ambient air pollution: A global assessment of exposure and burden of disease. Geneva, Switzerland. https://apps.who.int/iris/bitstream/10665/250141/1/9789241511353-eng.pdf.

Ying, Q., 2011. Physical and chemical processes of wintertime secondary nitrate aerosol formation. Front. Environ. Sci. En., 5, 348–361. https://doi.org/10.1007/s11783-011-0343-1.

Table 1. Summary of carbonaceous species concentrations.

Species	Unit	Campaign_1†		Campaign_2†	
		Winter	Summer	Sharif	Setad
OC	$\mu g/m^3$	7.8 (3.1–14.6)	6.8 (4.7–11.3)	11.4 (2.5–49.4)	9.8 (2.1–31.8)
EC	$\mu g/m^3$	3.5 (0.9–6.6)	3.5 (1.7–7.0)	2.7 (0.6–6.2)	2.0 (0.2–9.1)
OC/EC		2.5 (1.4–7.1)	2.1 (1.1–3.8)	4.9 (1.6–23.9)	8.0 (1.3–25.1)
∑PAHs	ng/m^3	8.0 (1.3–17.6)	3.1 (1.2–7.2)	6.3 (0.6–20.5)	5.0 (0.6–29.4)
∑Anhydrous sugars	ng/m^3	99.5 (11.3–219.0)	26.6 (0.5–155.7)	93.7 (6.8–377.7)	50.0 (5.6–325.1)
∑Hopanes	ng/m^3	7.1 (2.2–22.7)	5.5 (3.0–14.4)	8.5 (0.5–31.7)	6.9 (0.7–22.0)
∑n-Alkanes	ng/m^3	52.8 (13.4–115.8)	29.6 (11.3–41.3)	41.1 (4.8–98.0)	51.6 (6.8–170.7)

† Arithmetic mean (range)

Table 2. Summary of $PM_{2.5}$ source apportionment studies in Tehran.

Author (year)	Studied time interval	Method	Analyzed species	Identified sources (contribution)
Shahbazi et al. (2016)	Year 2013	Emission inventory	–	Mobile sources (69.9%) Energy conversion (19.9%) Industries (7.1%) Household, Commercial (2.4%) Transportation terminals (0.7%)
Arhami et al. (2017)	February 2014 to February 2015	24-hour $PM_{2.5}$ filter samples, collected at one residential site, PCA analysis	OC, EC, Inorganic ions, Crustal and non-crustal elements, Dust oxides, Sea salt	Re-suspended soil (48%) Heavy fuels combustion, metal abrasion and tire wears, lubricating oil and local industries (18%) Light duty vehicular sources (7%) Local industries (4%) Heavy duty vehicles (4%) Unexplained (19%)
Arhami et al. (2018)	February 2014 to February 2015	24-hour $PM_{2.5}$ filter samples, collected at one residential station, CMB analysis	OC, EC, Inorganic ions, Monthly averaged organic markers	Mobile sources (40%) Dust (24%) Sulfate (11%) Ammonium (5%) Nitrate (2%) Wood smoke (2%) Vegetative detritus (2%) Other OM (8%) Unidentified (5%)
Taghvaee et al. (2018)	May 2012 to June 2013	24-hour $PM_{2.5}$ filter samples, collected at two residential sites, PMF analysis	Inorganic ions, Crustal and non-crustal elements	Vehicular emissions (49.3% / 48.8%) Secondary aerosol (24.0% / 28.1%) Biomass burning (16.0% / 3.0%) Soil (8.2% / 2.8%) Industrial emissions (1.8% / 17.4%) Road dust (<1%)

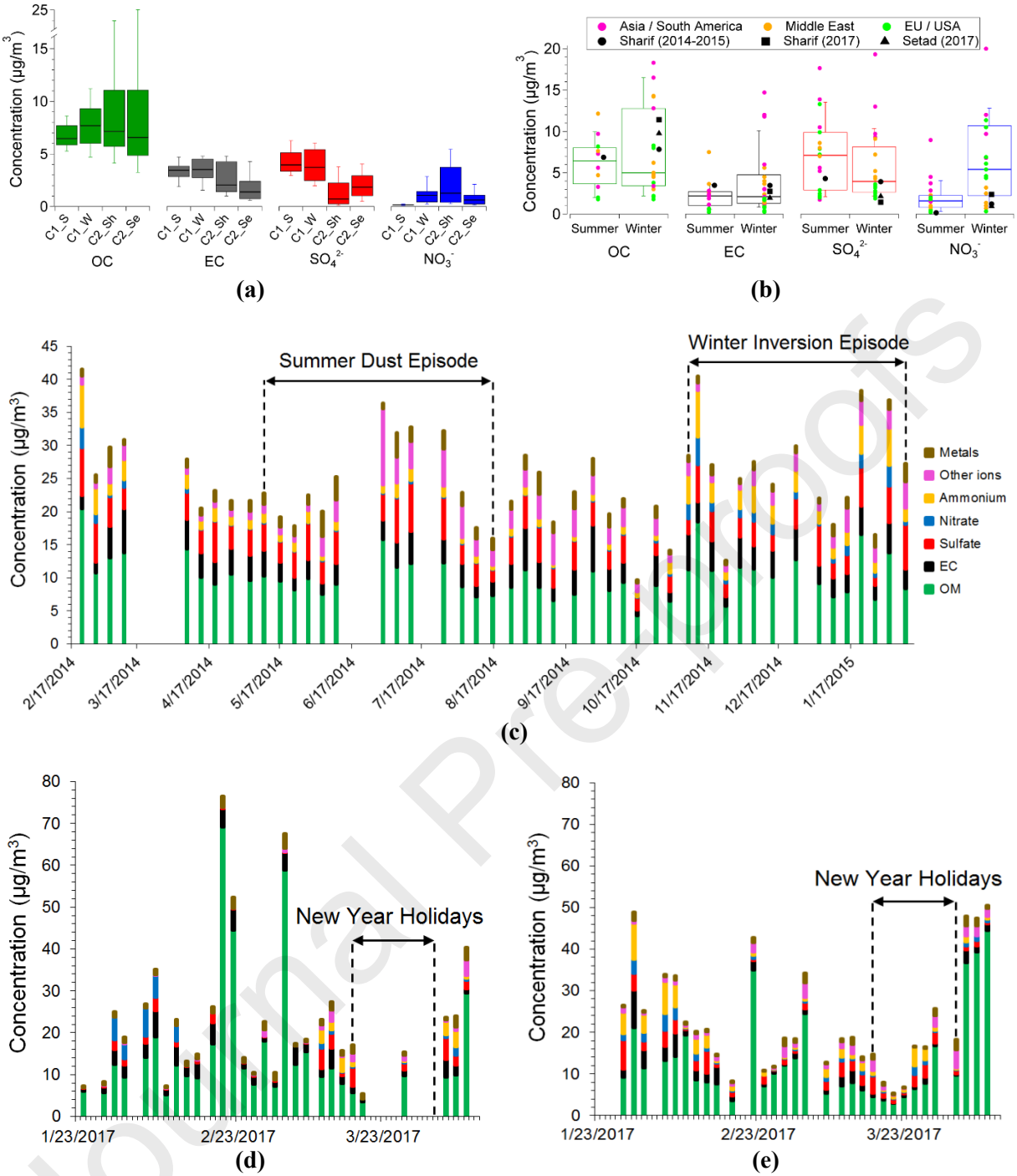

Figure 1. Comparison of OC, EC, sulfate and nitrate concentrations (a) among different sites and campaigns of this study and (b) with other parts of the world. Box-and-whiskers plots show the median, 25th and 75th percentiles, as well as 10th and 90th percentiles. (C1_S: Campaign_1 (Summer); C1_W: Campaign_1 (Winter); C2_Sh: Campaign_2 (Sharif); C2_Se: Campaign_2 (Setad)). Bulk chemical composition of the fine particulate matter samples collected at (c) Sharif site during Campaign_1, (d) Sharif site during Campaign_2 and (e) Setad site during Campaign_2.

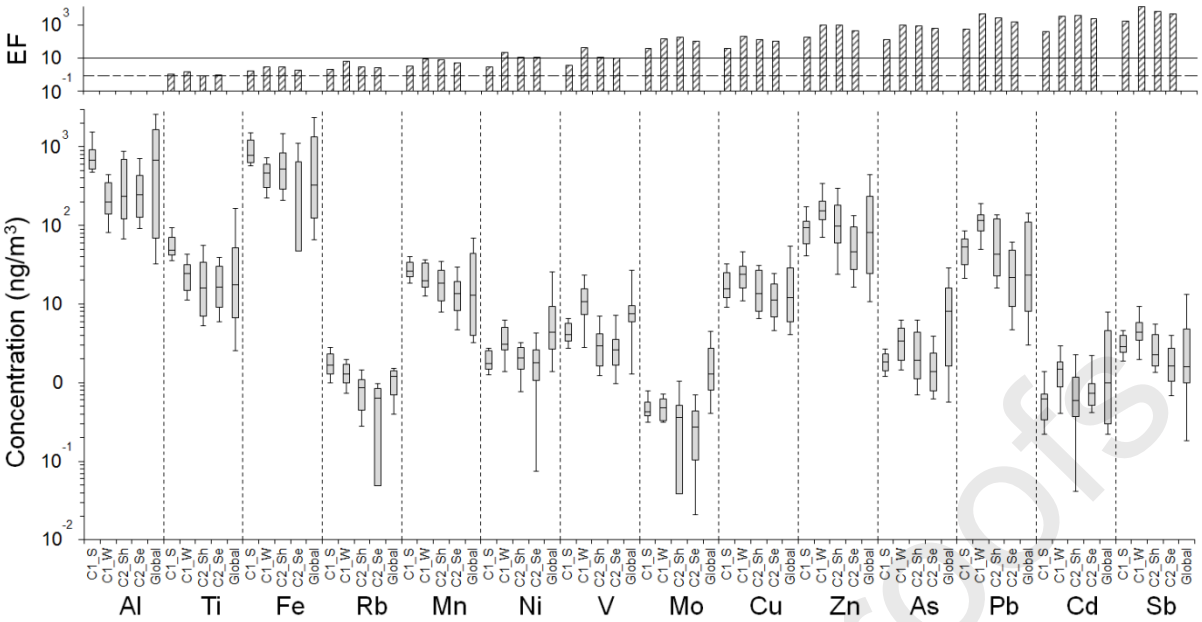

Figure 2. Comparison of mean enrichment factors (top) and element concentrations (bottom) among different sites and campaigns of this study and other parts of the world. Box-and-whiskers plots show the median, 25th and 75th percentiles, as well as 10th and 90th percentiles. (C1_S: Campaign_1 (Summer); C1_W: Campaign_1 (Winter); C2_Sh: Campaign_2 (Sharif); C2_Se: Campaign_2 (Setad)). EF = 1 and EF = 10 lines are also shown as reference.

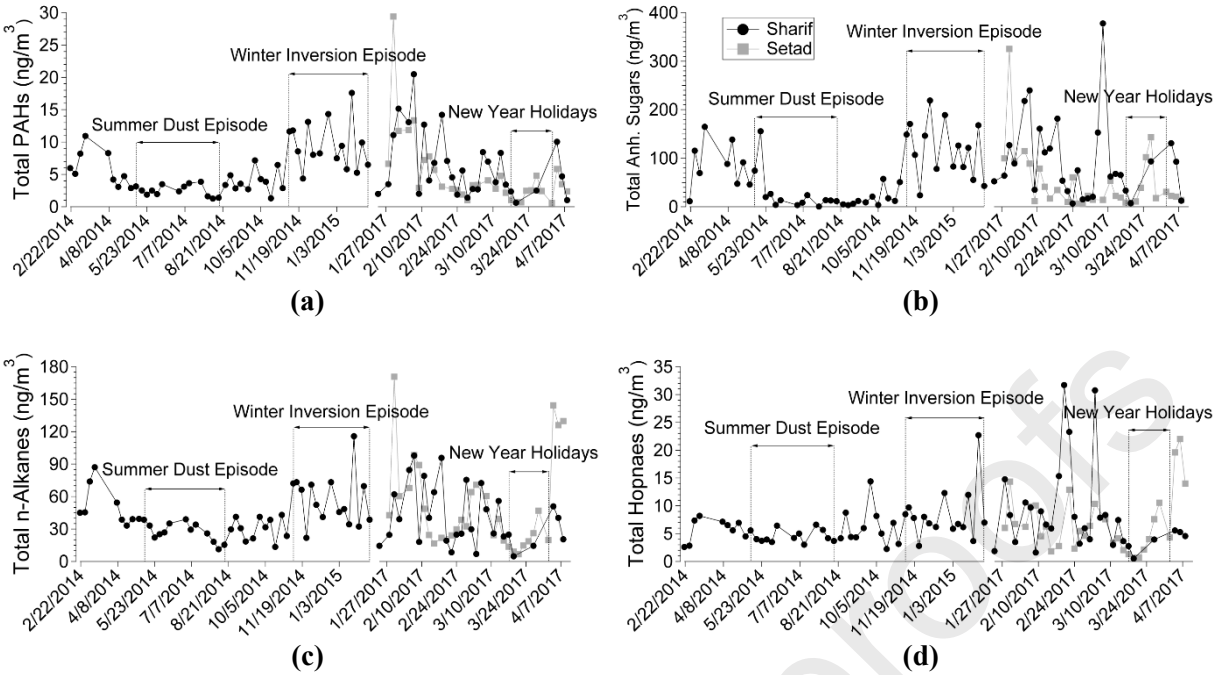

Figure 3. Time series of (a) ∑PAHs, R^2 = 0.63, (b) ∑Anhydrous sugars, R^2 = 0.08, (c) ∑n-Alkanes, R^2 = 0.03 and (d) ∑Hopanes, R^2 = 0.03, measured at each site for the two study campaigns. The R^2 values are the square of the Pearson correlation coefficient between the Sharif and Setad sites in Campaign_2.

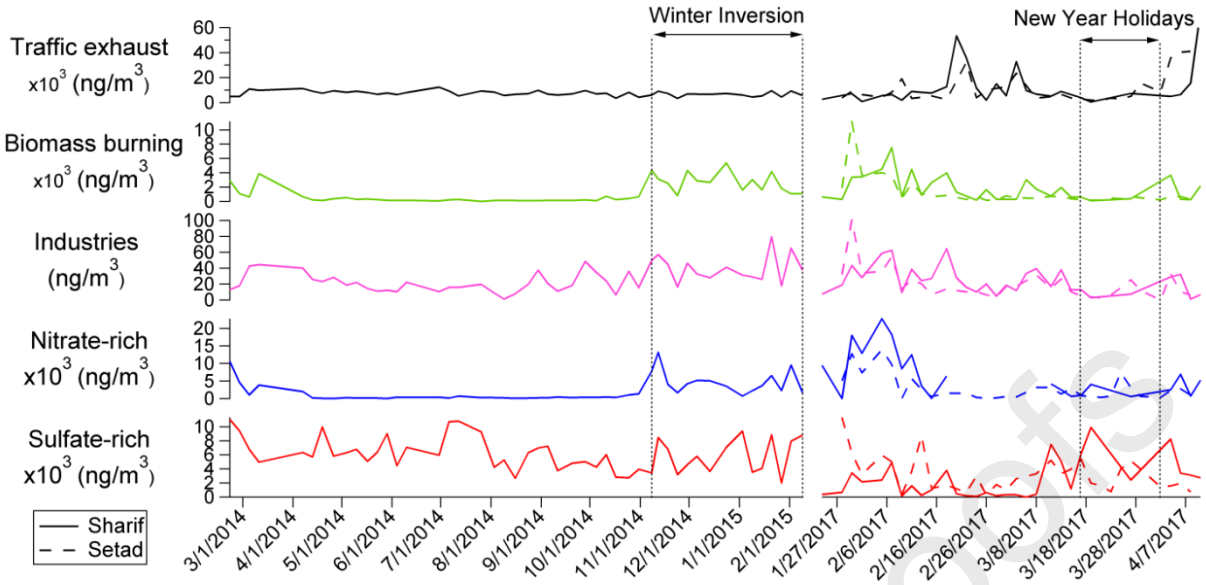

Figure 4. Time trends of the resolved factors from Marker-PMF. Solid lines represent the Sharif site and dashed lines represent the Setad site.

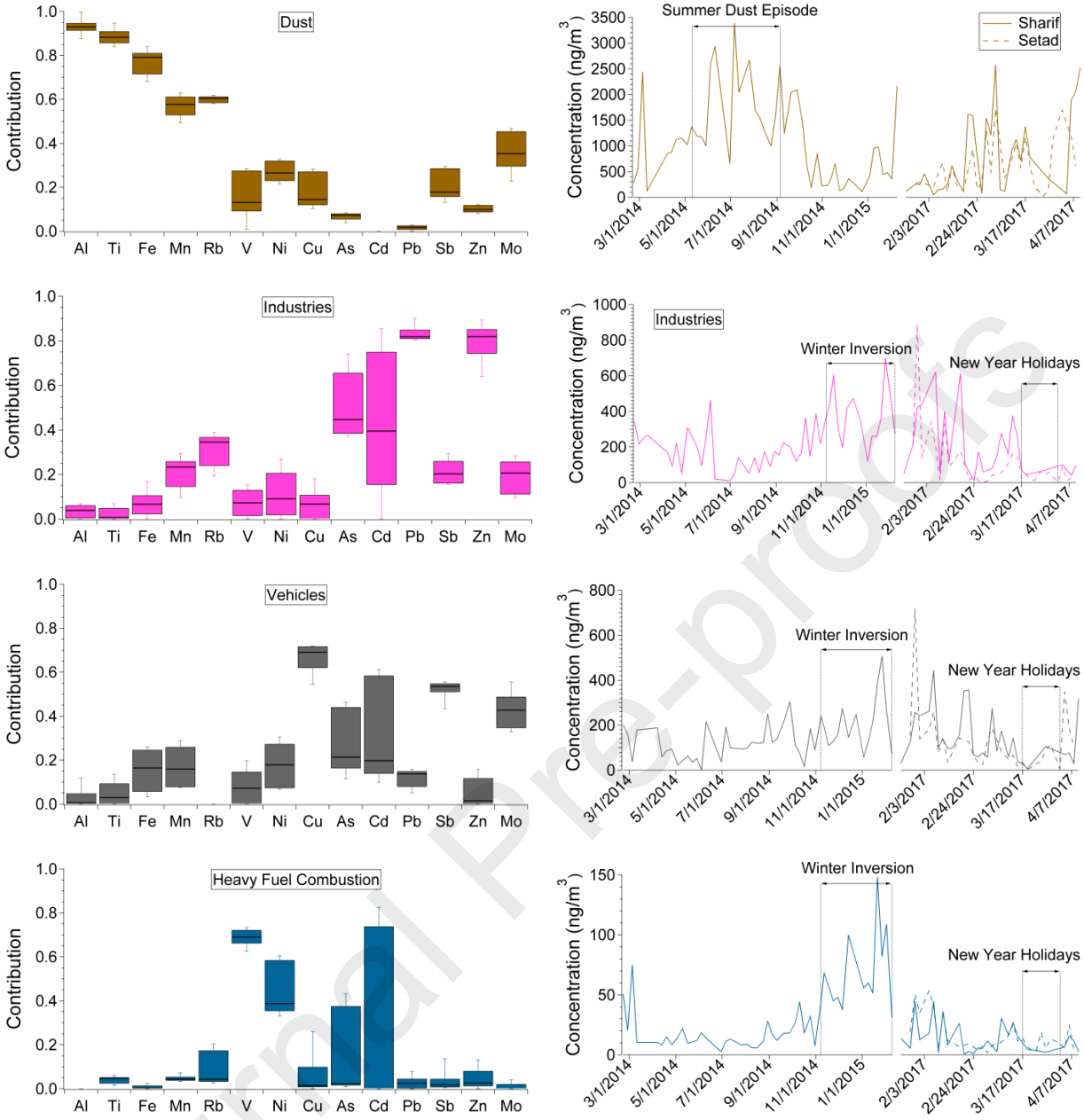

Figure 5. Relative contributions of the Metal-PMF factors to the measured variables, as box-and-whiskers (on the left) and their average time trends (on the right). Solid lines represent the Sharif site and dashed lines the Setad site. The boxes denote median, 25th and 75th percentiles, and the whiskers denote the 10th and 90th percentiles.

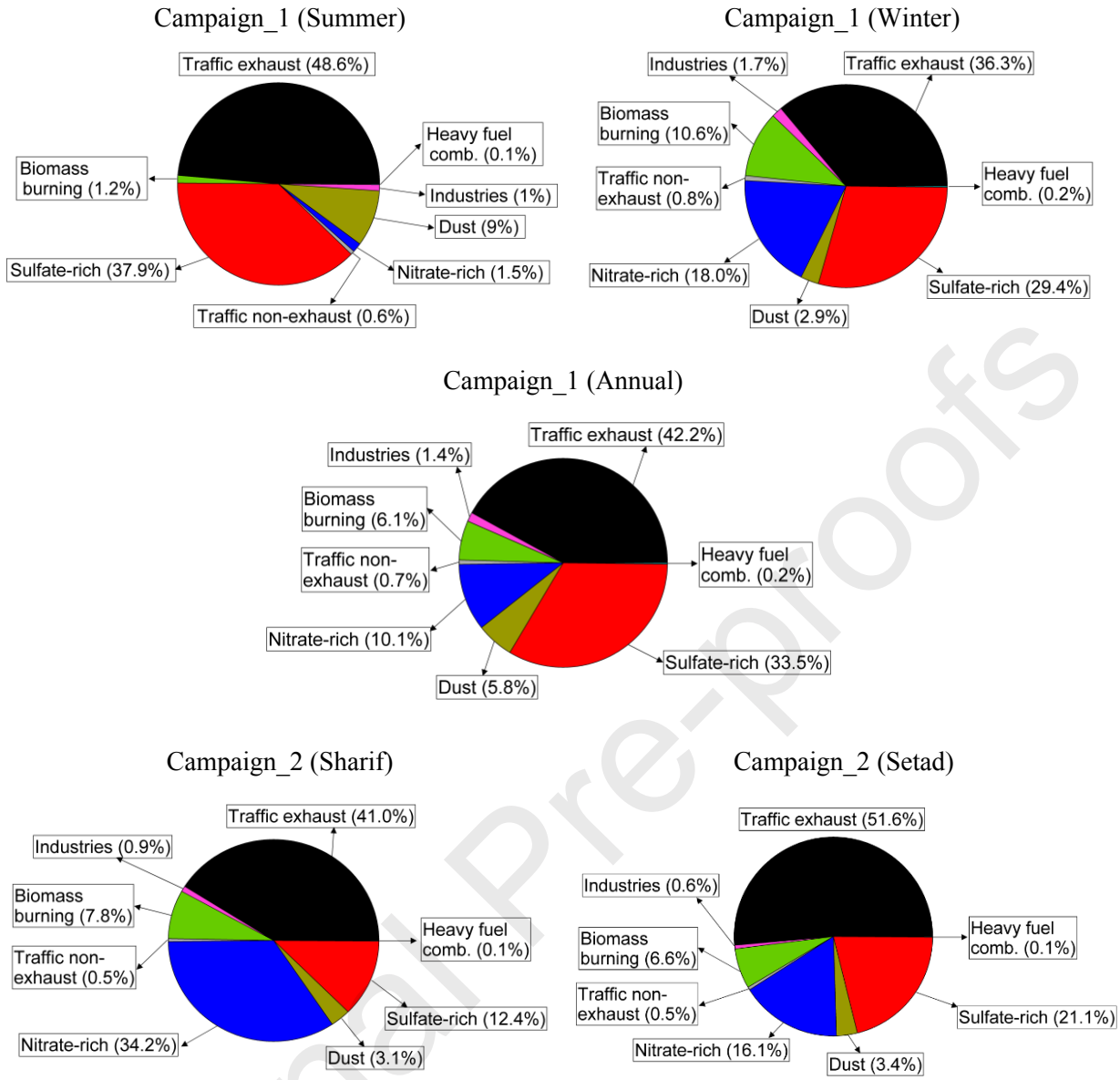

Figure 6. Mean contributions of the 8 identified sources to total $PM_{2.5}$ mass for each site and campaign. Here, the "Industries" factor is the sum of industrial sources resolve from Metal-PMF and Marker-PMF.

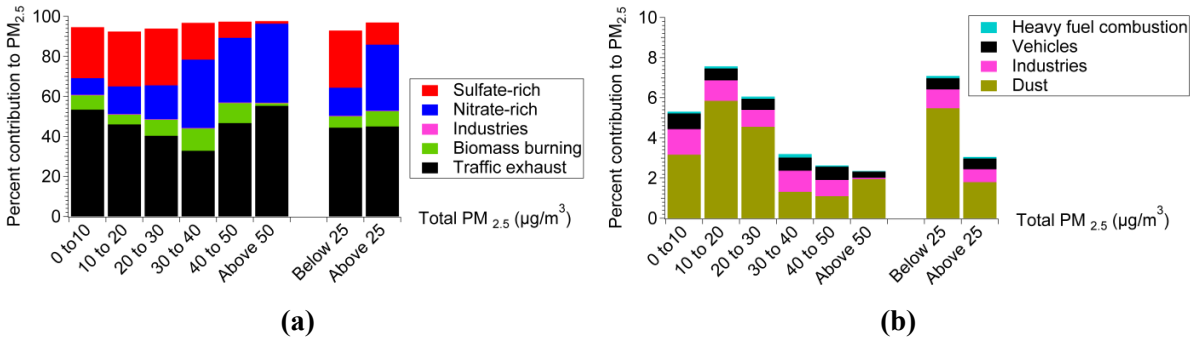

Figure 7. Contribution of the identified sources (%) to total $PM_{2.5}$ mass, distributed across different $PM_{2.5}$ concentration bins. (a) Marker-PMF, (b) Metal-PMF. (No. of samples in each bin are as following: 0 to 10 $\mu g/m^3$: 8 samples; 10 to 20 $\mu g/m^3$: 44 samples; 20 to 30 $\mu g/m^3$: 35 samples; 30 to 40 $\mu g/m^3$: 9 samples; 40 to 50 $\mu g/m^3$: 8 samples; Above 50 $\mu g/m^3$: 5 samples; Below 25 $\mu g/m^3$: 77 samples; Above 25 $\mu g/m^3$: 32 samples.)

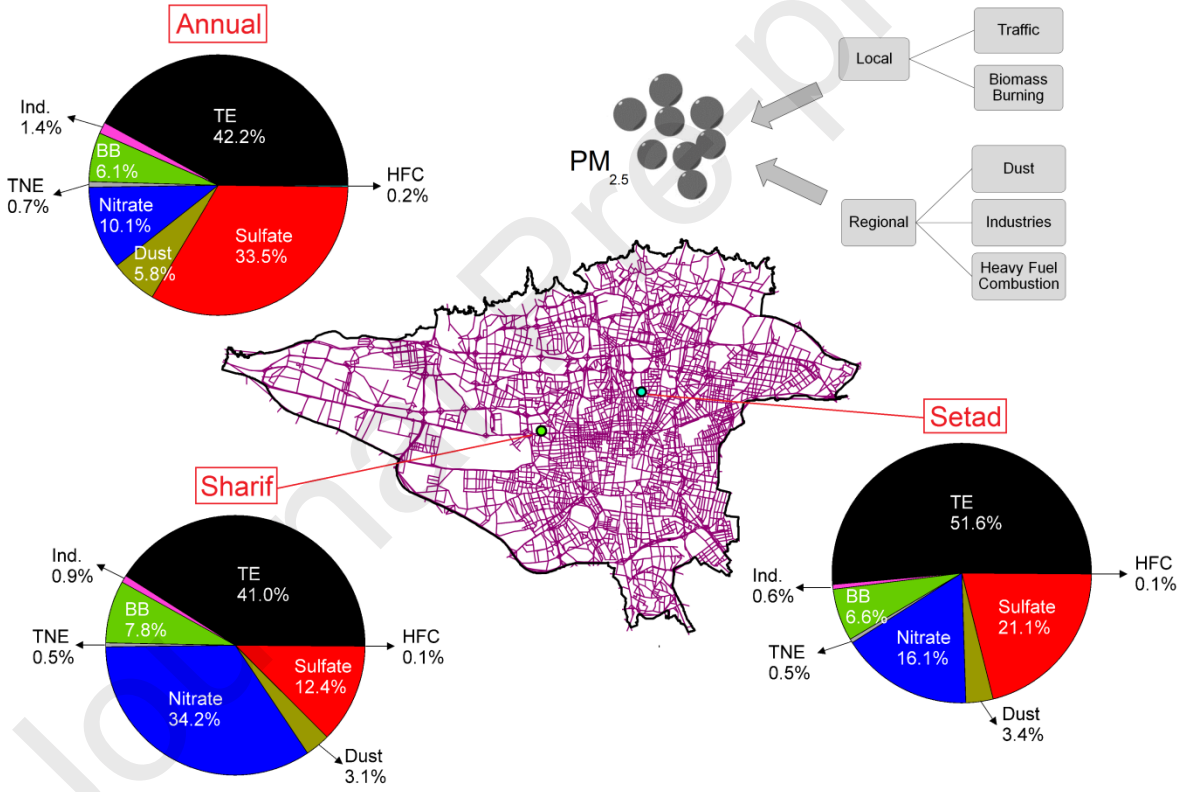

- Quantified $PM_{2.5}$ components in Tehran and PMF was used for source apportionment.
- Major $PM_{2.5}$ mass constituents were organic matter, sulfate and EC.
- 8 identified factors were: TE, BB, Ind., nitrate, sulfate, dust, TNE, and HFC.
- TE had 45% contribution to $PM_{2.5}$ mass. Sulfate and nitrate were the next major contributors.
- TE and BB were local sources, whereas dust, Ind. and HFC were regional sources.

Declaration of interests

☒ The authors declare that they have no known competing financial interests or personal relationships that could have appeared to influence the work reported in this paper.

☐The authors declare the following financial interests/personal relationships which may be considered as potential competing interests: